ARL-TR-7655 ● APR 2016

US Army Research Laboratory

A Skeletal, Gas-Phase, Finite-Rate, Chemical Kinetics Mechanism for Modeling the Deflagration of Ammonium Perchlorate—Hydroxyl-Terminated Polybutadiene Composite Propellants

by Chiung-Chu Chen and Michael McQuaid

NOTICES

Disclaimers

The findings in this report are not to be construed as an official Department of the Army position unless so designated by other authorized documents.

Citation of manufacturer's or trade names does not constitute an official endorsement or approval of the use thereof.

Destroy this report when it is no longer needed. Do not return it to the originator.

ARL-TR-7655 ● APR 2016

US Army Research Laboratory

A Skeletal, Gas-Phase, Finite-Rate, Chemical Kinetics Mechanism for Modeling the Deflagration of Ammonium Perchlorate—Hydroxyl-Terminated Polybutadiene Composite Propellants

by Chiung-Chu Chen and Michael McQuaid
Weapons and Materials Research Directorate, ARL

REPORT DOCUMENTATION PAGE

Form Approved
OMB No. 0704-0188

1. REPORT DATE *(DD-MM-YYYY)*	2. REPORT TYPE	3. DATES COVERED (From - To)
2016	Final	October 2014–January 2016

4. TITLE AND SUBTITLE
A Skeletal, Gas-Phase, Finite-Rate, Chemical Kinetics Mechanism for Modeling the Deflagration of Ammonium Perchlorate—Hydroxyl-Terminated Polybutadiene Composite Propellants

5a. CONTRACT NUMBER

5b. GRANT NUMBER

5c. PROGRAM ELEMENT NUMBER

6. AUTHOR(S)
Chiung-Chu Chen and Michael McQuaid

5d. PROJECT NUMBER
622618H80 PE # RK16

5e. TASK NUMBER

5f. WORK UNIT NUMBER

7. PERFORMING ORGANIZATION NAME(S) AND ADDRESS(ES)
US Army Research Laboratory
ATTN: RDRL-WML-D
Aberdeen Proving Ground, MD 21005-5069

8. PERFORMING ORGANIZATION REPORT NUMBER
ARL-TR-7655

9. SPONSORING/MONITORING AGENCY NAME(S) AND ADDRESS(ES)

10. SPONSOR/MONITOR'S ACRONYM(S)

11. SPONSOR/MONITOR'S REPORT NUMBER(S)

12. DISTRIBUTION/AVAILABILITY STATEMENT
Approved for public release; distribution is unlimited.

13. SUPPLEMENTARY NOTES

14. ABSTRACT
A (full) detailed, gas-phase, finite-rate chemical kinetics mechanism for representing the combustion-chemistry-associated ammonium perchlorate–hydroxyl-terminated polybutadiene (AP-HTPB) composite propellant deflagration was reduced to skeletal sets via the trial mechanism method. The full mechanism had 2,627 elementary reaction steps and involved 637 species. The primary objective of the effort was to produce a mechanism with 100 or fewer reactions and involving 100 or fewer species that could be employed as a submodel in computational fluid dynamics frameworks. Results produced by trial mechanism–homogeneous reactor (HR) model combinations were the basis for eliminating reactions. The choice of HR simulations to employ as the basis for mechanism reduction and candidate selection is discussed. Postreduction analyses were conducted to identify candidates with the best ability to mimic the full mechanism in AP-HTPB deflagration simulations at pressures from 300 to 20,000 psia. The candidate considered to offer the best compromise between size and mimicking ability for this purpose had 100 reactions and involved 81 species. The data comprising it are provided. Burning-rate estimates obtained with the mechanism provide additional evidence of its validity for AP-HTPB deflagration modeling.

15. SUBJECT TERMS
ammonium perchlorate, composite propellant, rocket propulsion, deflagration modeling, chemical kinetics

16. SECURITY CLASSIFICATION OF:			17. LIMITATION OF ABSTRACT	18. NUMBER OF PAGES	19a. NAME OF RESPONSIBLE PERSON
a. REPORT	b. ABSTRACT	c. THIS PAGE			Chiung-Chu Chen
Unclassified	Unclassified	Unclassified	UU	76	19b. TELEPHONE NUMBER (Include area code) 410-278-6185

Contents

List of Figures

List of Tables

Acknowledgments

Mr Todd Dutton and Dr Jeffrey Veals of the US Army Research Laboratory reviewed the initial manuscript and offered a number of suggestions that led to its improvement.

1. Introduction

To understand the deflagration of ammonium perchlorate–hydroxyl-terminated polybutadiene (AP-HTPB) composite propellants at a fundamental level, US Army Research Laboratory (ARL) researchers have built models to simulate the process (Chen and McQuaid 2014; McQuaid and Chen 2014; Nusca 2014). Of particular interest is the mechanism (or mechanisms) underlying the abrupt change in the slope of the burning rate (r_b) versus pressure. This phenomenon, which typically occurs around 3,000 psia (Atwood et al. 1999) and is referred to as an "exponent break," limits the performance potential of this propellant class (Atwood et al. 2013).

At the start of our efforts (in 2012), we found that the best available finite-rate chemical kinetics mechanism for modeling the gas-phase reaction chemistry associated with AP's combustion had a number of questionably parameterized rate expressions that sensitivity analyses indicated were important. Addressing this issue through the application of computational-chemistry-based methods and thermochemical kinetic theories, we developed and validated a gas-phase finite-rate chemical kinetics mechanism for modeling the combustion of pure AP (Chen and McQuaid 2014). That mechanism has since been updated and integrated with a previously built chemical kinetics mechanism for the combustion of HTPB (R45M polymer) in an NO_x-rich environment (Chen and McQuaid 2009; Chen and McQuaid 2010), producing a mechanism for modeling the combustion chemistry associated with AP-HTPB deflagration. It has (at present) 2,627 elementary reactions and involves 637 species. Some details of the estimation of reaction-rate expressions and thermochemical property estimates that were developed specifically for this mechanism have been presented (Chen and McQuaid 2015).

Because simulation run times would be prohibitively long and memory requirements excessive, it is not practical to employ the full AP-HTPB mechanism as a submodel in computational fluid dynamics (CFD) frameworks that our group employs to simulate deflagration phenomena (McQuaid and Chen 2014; Nusca 2014). Therefore, the trial mechanism method (TMM) invented by Kotlar (2010) and further developed by McQuaid (2013) was employed to produce (reduced) skeletal sets. With an objective of producing a mechanism with 100 or fewer reactions and involving 100 or fewer species to study exponent break phenomena, screening criteria were established to indicate a candidate's ability to mimic the full mechanism in models representing the deflagration of AP-HTPB mixtures having from 80- to 90-wt% AP. The pressure range of primary interest was 1,000–10,000 psia.

As in previous mechanism reduction efforts based on the TMM (Kotlar 2010; McQuaid 2013; McQuaid and Chen 2014), results of homogeneous reactor (HR) model simulations produced with trial mechanisms were employed as bases for eliminating reactions. However, the implementation of the method was not as straightforward as it was in the past. Because AP-HTPB propellants have composite/nonhomogeneous structure, there are regions near the condensed-phase-gas-phase interface that are very rich in the daughters of HTPB's pyrolysis and others that are rich in the daughters of AP's decomposition (Surzhikov and Krier 2003; Gross et al. 2013). As such, there was a desire to screen trial mechanisms on the basis of simulations with starting chemical compositions that ranged from the nascent product distributions for the condensed-phase to gas-phase conversion of (pure) AP to the nascent product distribution for the condensed-phase to gas-phase conversion of (pure) HTPB (R45M polymer) (Surzhikov and Krier 2003; Gross et al. 2013). Vetting trial mechanisms at a number of different pressures over the range of interest was also desired. However, because the run times of relevant simulations were relatively long, the number of simulations that could be employed for screening was extremely limited. Since that limited the parameter space within which candidates produced by the TMM could be expected to be valid, it prompted us to make some assumptions about the relative importance of various subprocesses and to apply the method in stages. Specifics of the implementation, including some deviations from past practice, are discussed.

Postreduction analyses were conducted to identify candidates with the best potential to mimic the full mechanism in intended applications. Of the candidates with the potential to be a submodel for the ARL CFD laminate framework (Nusca 2014), the one considered to be the best compromise between size and ability to mimic the full mechanism within the delineated parameter space had 100 reactions and involved 81 species. Results from simulations that were the basis for mechanism reduction and candidate selection are presented. Burning rate estimates for homogeneous AP and AP-HTPB systems produced with a 1-dimensional (1-D), 2-phase, premixed laminar flame (CYCLOPS) model provide additional evidence for the mechanism's validity for intended applications.

2. Implementation of the Trial Mechanism Method

More complete descriptions of the TMM are given elsewhere (Kotlar 2010; McQuaid 2013). Steps include the following:

- Randomly ordering the full mechanism's reactions/rate expressions.
- Sequentially eliminating single reaction rate expressions from it on a trial basis.

- Rerunning constant-pressure (CONP) HR simulations with the (trial) mechanism created by the elimination.
- Permanently eliminating the reaction/rate expression if none of the changes to selected results of the simulations exceed specified criteria.

A species is eliminated as a consequence of all the reactions involving it being eliminated.

As in previous efforts (Kotlar 2010; McQuaid 2013; McQuaid and Chen 2014), parameters of the simulations that were compared were local maxima found in mass-specific and volumetric "heat release rate" ($\dot{q}_{mass}^{max}$ and $\dot{q}_{vol}^{max}$, respectively) versus time (t) traces, the times at which those maxima occurred (t_{mass}^{max} and t_{vol}^{max}, respectively), and the temperature at the final time step of the simulation (T_f). In contrast to the efforts by Kotlar (2010) and McQuaid (2013), however, $\dot{q}_{mass}$ and $\dot{q}_{vol}$ were calculated per

$$\dot{q}_{mass}(t) = R\left(T(t) * \sum_k \frac{dY_k(t)}{dt}/W_k + \frac{dT(t)}{dt} * \sum_k Y_k(t)/W_k\right) \quad (1a)$$

and

$$\dot{q}_{vol}(t) = \rho_g(t) * \dot{q}_{mass}(t), \quad (1b)$$

where R is the universal gas constant, T is the temperature, Y_k is the mass fraction of the k^{th} species, W_k is its molecular weight, and ρ_g is the gas mixture's density. This approach was developed in the course of a prior effort to avoid numerical instabilities that occasionally arose when $\dot{q}_{mass}$ and $\dot{q}_{vol}$ were computed on the basis of species' chemical production rates and their enthalpies (McQuaid and Chen 2014). Traced to poorly formulated/"spliced" coefficients employed for calculating species' enthalpies, that issue has been resolved and does not apply to the current AP-HTPB mechanism. However, since screening based on Eqs. 1a and 1b is as effective and is less computationally expensive than the previous method, there was no reason to return to prior practice.

Following the same reaction step order (minus those that had been eliminated), the screening process was repeated for a given set of acceptance criteria if at least one reaction was permanently eliminated in the course of a complete pass through the mechanism. When no more reactions could be eliminated without exceeding any specified tolerance, or 10 complete passes at a specified set of tolerances had been completed, the tolerances were relaxed and the process repeated.

The HR model employed to perform the simulations used the CHEMKIN-II subroutine library (Kee et al. 1989). Solutions for the model's differential-algebraic equations were obtained with DASPK (Li and Petzold 2000). For the reductions reported here, the tolerances for variations in q_{vol}^{max}, q_{mass}^{max}, t_{vol}^{max}, and t_{mass}^{max} were

set at ±1.0 % for the first pass. The tolerance for variation in T_f was set at ±1.0 K. They were subsequently relaxed in ±1.0%–±1.0 K increments. The largest tolerances employed were ±10% and ±10 K. Collectively they are referred as the ±10%–±10 K acceptance criteria. As will be discussed, the bases for these criteria are empirical and not foolproof. Thus postreduction analyses are an integral aspect of candidate selection. In the present case, they were needed to address issues that arose because trial mechanisms could not be screened (initially) on the basis of simulations that covered the entire parameter space considered relevant.

Table 1 shows the input parameters for sets of HR simulations that were employed for the reduction effort. Starting with set A (and evolving from B, to C, to D as the effort progressed), they were based on observations pertaining to AP-HTPB composite propellants and their deflagration.

Table 1 Input parameters for CONP HR simulations employed for the initial reduction of the full mechanism

Set	Start[a]	Comp.[b]	Sim.	Wt% AP	Wt% HTPB	Initial Temp. (K)	Pressure (psia)	Sim. Length (s)
A	96	25	1	100	0	900	3,000	1.0000
			2	80	20	900	3,000	5.0000
B	48	>11[c]	1	100	0	900	1,000	0.2000
			2	80	20	900	1,000	0.0100
C	48	29	1	100	0	900	1,000	0.2000
			2	80	20	900	1,000	0.0100
			3	80	20	900	10,000	0.0015
D	48	7	1	100	0	900	1,000	0.2000
			2	80	20	900	1,000	0.0100
			3	80	20	900	10,000	0.0015
			4	100	0	900	10,000	0.0060

[a]Number of reductions with different reaction orderings that were started.
[b]Number of different reaction orderings for which at least one pass through the full mechanism was completed and a workable reduced mechanism was produced.
[c]Some files were inadvertently deleted, and the actual number of orderings that produced at least one reduced mechanism is no longer known but it was greater than 11.

As in prior efforts (Kotlar 2010; McQuaid 2013; McQuaid and Chen 2014), the starting chemical compositions were chosen to reflect expectations for the nascent products of the condensed-phase to gas-phase conversion process of individual propellant ingredients, in this case AP and HTPB. For the nascent product of AP's decomposition, an NH_3-$HClO_4$ complex (labeled NH_4ClO_4) was chosen based on prior work (McQuaid and Chen 2014). In that work, an earlier version of the full mechanism discussed in this report was reduced and a resultant mechanism employed with the CYCLOPS framework to calculate pure AP's burning rate as a function of pressure. Finding conflicting evidence as to the nature of the nascent product(s) of the condensed-phase to gas-phase conversion process—with either

NH_4ClO_4 or NH_3 + $HClO_4$ being the primary candidates—we compared burning-rate estimates produced by them individually. The difference was found to be negligible. The decision to employ NH_4ClO_4 instead of NH_3 + $HClO_4$ (or some combination of the 2) was made because NH_4ClO_4 was more "condensed-phase-like" and it was easy to imagine it as a transitional state for AP's decomposition. Burning-rate estimates that were in reasonable agreement with measured values affirmed the choice.

A relatively large hydrocarbon ($C_{20}H_{32}$) with the same ratio of cis/trans/vinyl butadiene substructures as R45M polymer was chosen as the nascent product of HTPB's pyrolysis. Labeled R45M, CYCLOPS-based calculations that employed it as the nascent product of HTPB's thermally induced decay were found to yield rates that were in good agreement with measured values (Chen and McQuaid 2009).

The choice of NH_4ClO_4:R45M concentration ratios to use to start the HR simulations was less straightforward. The relative weight of AP in AP-HTPB formulations (without aluminum) is typically in the range from 80% to 90% (Cai et al. 2008; Hedman et al. 2012, Gross et al. 2013). However, as mentioned in the Introduction, the range of fuel-oxidizer ratios in the gas phase near the surface of a burning composite propellant is much broader than that. Being composite/nonhomogeneous, there are regions near the surface that are very rich in the daughters of HTPB's pyrolysis and others that are rich in the daughters of AP's decomposition (Surzhikov and Krier 2003; Gross et al. 2013). As such, to increase the probability that the method would produce candidates that were valid over the entire pertinent range, simulations with starting compositions that ranged from 100% NH_4ClO_4 to 100% R45M would normally have been employed for screening. However, for the TMM to be practical, one complete pass through the full mechanism needs to be complete in less than 168 h (1 week) of central processing unit time, and that forced some compromises. The CONP simulations chosen as the basis for the reduction proved to have run times of 2–5 min when the HR model was equipped with the full mechanism, and the full mechanism had 2,627 reactions. Therefore, a single pass through the mechanism had the potential to take more than a week when just one simulation was employed for the screening process. (Simulation times get shorter as reactions are eliminated. Thus the total time needed to complete a pass depends on the number of reactions that are eliminated, making a priori estimates for the time it will take to complete the first pass unreliable.) As such, the number of different simulations that could be employed as bases for the decision to eliminate a reaction was severely limited, preventing us from relying completely on the TMM to screen candidates over the entire composition range of interest. Rather, we needed to choose a restricted range over which to screen eliminations, then search for candidates that met acceptance criteria outside that range.

Given those considerations, we made some judgements about the relative importance of fuel-oxidizer ratios within the full range. First, we concluded that the single most important ratio to include would be for the 80-20 AP-HTPB case. Having an fuel-oxidizer equivalence ratio close to 1, this case would ensure that the process went to completion, and it was assumed it would be the one most likely to be able to produce a reduced mechanism that could represent the combustion chemistry over the entire range of compositions that are pertinent to the process.

Next, observing that the deflagration of pure AP is self-sustaining at pressures above 20 atm (300 psi) and that it is clearly an important subprocess in the deflagration of AP-HTPB composite propellants (Gross et al. 2011; Gross et al. 2013), we considered it important that the reduced mechanism be able to produce simulations that mimic those produced by the full mechanism for this composition. The complete decomposition/pyrolysis of 100-wt% HTPB in the absence of oxidizers, on the other hand, was assumed to be far less important. It is slow on the 1- to 10-ms time scale needed for the heat-up and conversion of a propellant into final products (Chen and McQuaid 2009). Thus, we did not consider it necessary that the results produced by a reduced mechanism meet the same criteria for modeling HTPB's pyrolysis as those for the stoichiometric to oxidizer-rich conditions. Based on these considerations, and not expecting that more than 2 simulations could be employed for screening, we chose 100-wt% NH_4ClO_4 as the starting composition for one simulation and 80-20-wt% NH_4ClO_4-R45M as the starting composition for the other.

For all the HR simulations performed in this effort the starting temperature was chosen to be 900 K. This choice stemmed from observations made in the course of reducing an earlier version of the AP (only) submechanism of the current full AP-HTPB mechanism and burning rate estimates for pure AP produced by PREMIX/CYCLOPS-based models (McQuaid and Chen 2014). In those efforts, pressure-dependent starting temperatures ranging from 800 to 1,200 K were chosen because published pyrolysis laws indicated that the surface temperature of deflagrating AP would be in this range and rise with pressure.

That said, the correspondence between the starting conditions for the HR simulations and the conditions employed in the CYCLOPS-based deflagration model was not as clear cut as imagined. Briefly, we have always assumed that one of the reasons HR simulations are an effective basis for producing reduced mechanisms for use in modeling combustion chamber dynamics and deflagration phenomena is that there is a fairly direct correspondence between the temporal dimension of HR simulations and the spatial dimension(s) of the gas-phase combustion of a burning propellant. However, in the present case there was a very rapid equilibration step between NH_4ClO_4 and NH_3 + $HClO_4$ in the HR simulation

that dropped the temperature more than 100 K within about 10^{-9} s. As will be discussed, nothing comparable happens in the spatial dimension of the 1-D flame simulations. Nevertheless, we found that the reduced mechanism derived on the basis of the aforementioned HR simulations yielded reasonable CYCLOPS-based estimates for the linear burning rate of pure AP. We also found that linear burning rates were effectively independent of the temperature that was specified for the surface (as dictated by a pyrolysis law) (McQuaid and Chen 2014). Thus, 900 K was deemed a reasonable choice to employ for all pressures.

Not expecting that more than 2 simulations would be able to be employed as bases for the (initial) reduction, and that one should have 80-20-wt% NH_4ClO_4-R45M as the starting composition and 100-wt% NH_4ClO_4 for the other, we decided to use one (intermediate) pressure for both, then search for candidates that would produce results similar to the full mechanism over the pressure range of particular interest: 1,000–10,000 psia. We chose 3,000 psia for the first attempt (set A) since exponent breaks generally occur near that value. However, that set did not produce a candidate that was able to reproduce a secondary ($t_{mass}^{max}, q_{mass}^{max}$) datum produced at 1,000 psia (Fig. 1.) The pressures specified for the simulations employed in sets B–D addressed this issue.

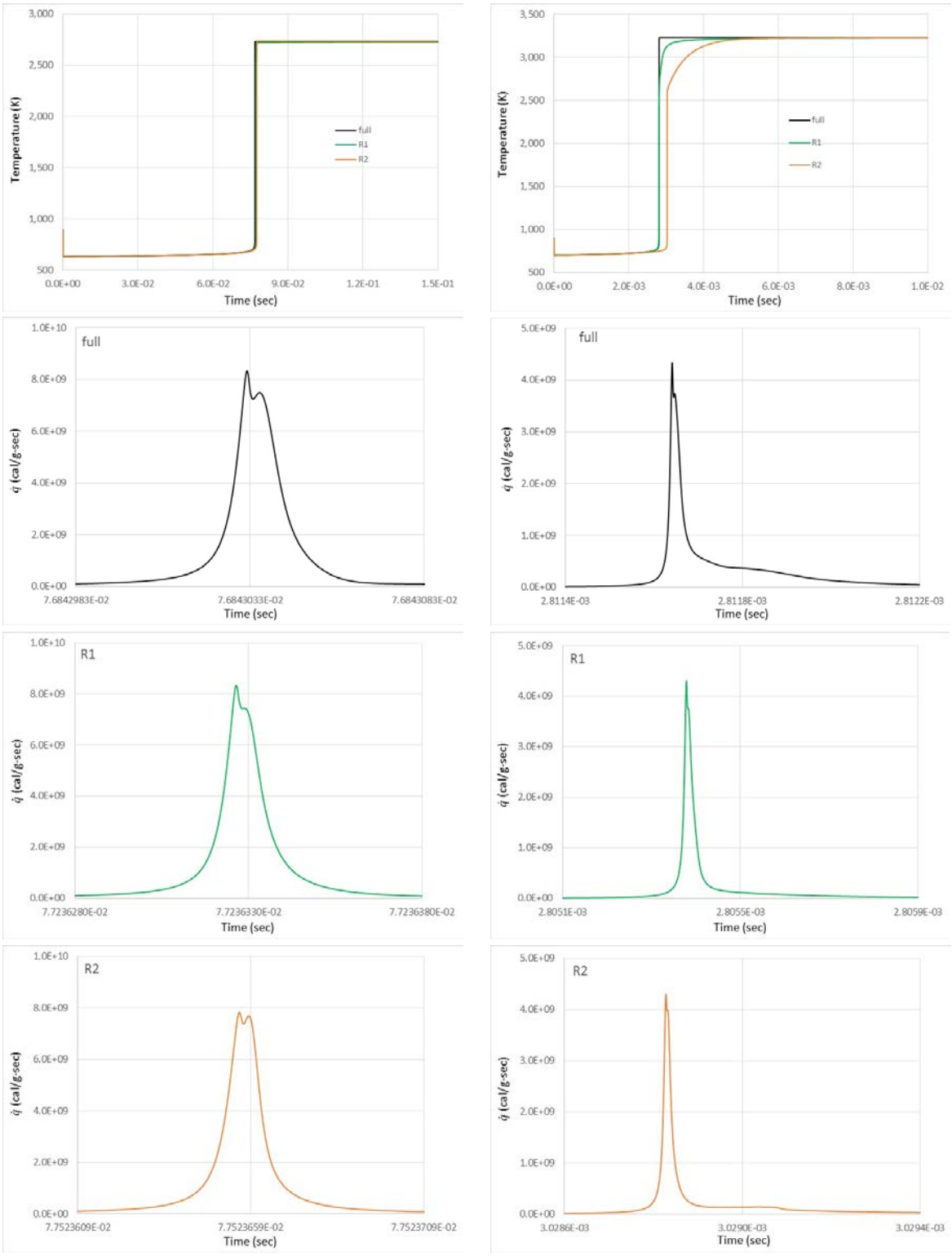

100 NH_4ClO_4 80-20 NH_4ClO_4-R45M

Fig. 1 Comparison of mass-specific heat release and temperature vs. time traces for CONP HR simulations produced with the full, R1, and R2 mechanisms; 1,000 psia

Considering it important that simulations approach an equilibrium state, we specified temporal durations for set A such that the temperature difference between the final 2 time steps of a simulation was effectively zero. However, with such durations employed, most of the reduced mechanisms that were produced generated *T* versus *t* traces that for *t* near the primary heat release event were by visual inspection in poor agreement with simulations produced by the full mechanism. The shorter durations of the simulations in sets B–D were specified to address this issue.

Candidates with 100 or fewer reactions and 100 or fewer species were produced by sets A–C. However, postreduction analyses based on visual inspection of full *T* versus *t* traces raised concerns about all of them. Therefore, *T* versus *t* traces meeting ±1.0%–±1.0 K acceptance criteria in sets A and B were visually inspected to identify candidates that might be suitable for further reduction with a wider set of screening criteria. That search led to the identification of a candidate from set B that produced traces that well-mimicked those produced by the full mechanism over the entire parameter space of interest. Referred to hereafter as R1, it had 203 reactions and involved 123 species.

Subsequent to R1's identification, a mistake in the full mechanism and R1 was identified and corrected. This change had a negligible impact on the *T* versus *t* traces produced by the full mechanism and R1. It did, however, result in R1 failing to produce 2 $\dot{q}_{mass}$ maxima in the AP-HTPB simulation at 1,000 psia. Appearing as a shoulder on the main feature of the $\dot{q}_{mass}$ versus *t* trace, the feature associated with the second maximum is clearly observed. Thus, this discrepancy was considered ignorable.

R1 was reduced based on the set of simulations whose input parameters are listed in Table 2. When postreduction analyses indicated a mechanism produced by its reduction met most of the criteria that were sought, the reduction effort was stopped. That mechanism is referred to hereafter as R2.

Table 2 Input parameters for CONP HR simulations employed for the reduction of R1

Set	Start[a]	Comp.[b]	Sim.	Wt% AP	Wt% HTPB	Initial temp. (K)	Pressure (psia)	Sim. length (s)
E	48	48	1	100	0	900	500	0.3000
			2	80	20	900	500	0.0120
			3	100	0	900	20,000	0.0015
			4	80	20	900	20,000	0.0006

[a]Number of reductions with different reaction orderings that were started.
[b]Number of different reaction orderings for which at least one pass through the full mechanism was completed and a workable reduced mechanism was produced.

3. Postreduction Analysis

The criteria employed in this effort for deciding whether a simulation produced by a trial mechanism was in good agreement with a simulation produced by the full mechanism are to a large extent the same as those that were employed by Kotlar (2010) in the first published application of the TMM. That application and subsequent ones have borne out their efficacy but they are not foolproof. Decisions to eliminate reactions are based on comparing (for each simulation) 1 or 2 data points from 3 different traces that usually have in excess of 1,000 data points each. Therefore, it is possible (and sometimes frequently observed) that, when plotted in their entirety and compared with the standard, simulations meeting all the acceptance criteria exhibit traits that raise concerns. Due to such "false positives", comparing the traces produced by candidates with those produced by the standard is a necessary aspect of candidate validation and selection. Nevertheless, to determine if HR simulations produced with R1 and R2 would meet the acceptance criteria employed in the reduction process over the entire parameter space of interest, a set of simulations that spanned the space were run and discrepancies identified. The set included simulations at pressures from 300 to 22,000 psia (20–1,500 atm). The results are shown in Tables 3 and 4.

Table 3 Comparison of parameters produced by the full and reduced mechanisms in CONP HR simulations in which the starting composition was 100-wt% NH_4ClO_4

Pressure (psia)	Parameter	Units	Full	R1	Δ	R2	Δ
300	$t_{vol/mass}^{max}$ [a]	seconds	4.123E-01	3.970E-01	–4%	3.236E-01	–21%
	$\dot{q}_{vol}^{max}$	cal/cm^3-s	1.427E+07	1.418E+07	–1%	1.316E+07	–8%
	$\dot{q}_{mass}^{max}(1)$	cal/g-s	2.415E+09	2.411E+09	0%	2.294E+09	–5%
	$\dot{q}_{mass}^{max}(2)$	cal/g-s	2.345E+09	2.277E+09	–3%	2.439E+09	+4%
	T_f(1 s)	K	2686	2685	–1 K	2686	0 K
500	$t_{vol/mass}^{max}$ [a]	seconds	2.073E-01	2.049E-01	–1%	2.050E-01	–1%
	$\dot{q}_{vol}^{max}$	cal/cm^3-s	4.039E+07	4.003E+07	–1%	3.693E+07	–9%
	$\dot{q}_{mass}^{max}(1)$	cal/g-s	4.149E+09	4.134E+09	0%	3.911E+09	–6%
	$\dot{q}_{mass}^{max}(2)$	cal/g-s	3.884E+09	3.798E+09	–2%	4.046E+09	+4%
	T_f(1 s)	K	2706 K	2705	–1 K	2706 K	0 K
1,000	$t_{vol/mass}^{max}$ [a]	seconds	7.670E-02	7.730E-02	+1%	8.386E-02	+9%
	$\dot{q}_{vol}^{max}$	cal/cm^3-s	1.557E+08	1.540E+08	–1%	1.416E+08	–9%
	$\dot{q}_{mass}^{max}(1)$	cal/g-s	8.336E+09	8.298E+09	0%	7.853E+09	–6%
	$\dot{q}_{mass}^{max}(2)$	cal/g-s	7.490E+09	7.453E+09	0%	7.863E+09	+5%
	T_f (1 s)	K	2730	2730	0 K	2730	0 K
3,000	$t_{vol/mass}^{max}$ [a]	seconds	1.457E-02	1.480E-02	+2%	1.639E-02	+12%
	$\dot{q}_{vol}^{max}$	cal/cm^3-s	1.243E+09	1.228E+09	–1%	1.128E+09	–9%
	$\dot{q}_{mass}^{max}$	cal/g-s	2.416E+10	2.340E+10	–3%	2.274E+10	–6%
	T_f(1 s)	K	2763	2764	+1 K	2764	+1 K
10,000	$t_{vol/mass}^{max}$ [a]	seconds	2.330E-03	2.333E-03	0%	2.576E-03	+11%
	$\dot{q}_{vol}^{max}$	cal/cm^3-s	1.238E+10	1.233E+10	0%	1.132E+10	–9%
	$\dot{q}_{mass}^{max}$	cal/g-s	7.591E+10	7.586E+10	0%	7.127E+10	–6%
	T_f(1 s)	K	2794	2796	+2 K	2796	+2 K
20,000	$t_{vol/mass}^{max}$ [a]	seconds	9.136E-04	9.025E-04	–1%	9.931E-04	+9%
	$\dot{q}_{vol}^{max}$	cal/cm^3-s	4.399E+10	4.451E+10	+1%	4.062E+10	–8%
	$\dot{q}_{mass}^{max}$	cal/g-s	1.399E+11	1.416E+11	+1%	1.313E+11	–6%
	T_f(1 s)	K	2810	2812	+2 K	2812	+2 K

[a]To the number of significant digits necessary to establish whether the acceptance criteria were met, t_{vol}^{max} and t_{mass}^{max} were the same.

Table 4 Comparison of parameters produced by the full and reduced mechanisms in CONP HR simulations in which the starting composition was 80-wt% NH_4ClO_4 and 20-wt% R45M

Pressure (psia)	Parameter	Units	Full	R1	Δ	R2	Δ
300	$t_{vol/mass}^{max}$ [a]	seconds	4.451E-03	4.473E-03	0%	4.684E-03	+5%
	$\dot{q}_{vol}^{max}$	cal/cm^3-s	8.961E+06	9.046E+06	+1%	8.238E+06	–8%
	$\dot{q}_{mass}^{max}(1)$	cal/g-s	1.286E+09	1.301E+09	+1%	1.230E+09	–4%
	$\dot{q}_{mass}^{max}(2)$	cal/g-s	1.207E+09	1.224E+09	+1%	1.236E+09	+2%
	T_f(1 s)	K	3143	3144	+1 K	3162	+19 K
500	$t_{vol/mass}^{max}$ [a]	seconds	3.796E-03	3.829E-03	+1%	3.949E-03	+4%
	$\dot{q}_{vol}^{max}$	cal/cm^3-s	2.503E+07	2.514E+07	0%	2.289E+07	–9%
	$\dot{q}_{mass}^{max}(1)$	cal/g-s	2.180E+09	2.195E+09	+1%	2.076E+09	–5%
	$\dot{q}_{mass}^{max}(2)$	cal/g-s	1.954E+09	1.988E+09	+2%	2.033E+09	+4%
	T_f(1 s)	K	3182	3184	+2 K	3202	+20 K
1,000	$t_{vol/mass}^{max}$ [a]	seconds	2.817E-03	2.829E-03	0%	2.859E-03	+1%
	$\dot{q}_{vol}^{max}$	cal/cm^3-s	9.461E+07	9.456E+07	0%	8.646E+07	–9%
	$\dot{q}_{mass}^{max}(1)$	cal/g-s	4.288E+09	4.302E+09	0%	4.094E+09	–5%
	$\dot{q}_{mass}^{max}(2)$	cal/g-s	3.666E+09	[b]	. . .	[b]	. . .
	T_f(1 s)	K	3228	3230	+2 K	3249	+21 K
3,000	$t_{vol/mass}^{max}$ [a]	seconds	1.393E-03	1.403E-03	+1%	1.376E-03	–1%
	$\dot{q}_{vol}^{max}$	cal/cm^3-s	7.341E+08	7.270E+08	–1%	6.739E+08	–8%
	$\dot{q}_{mass}^{max}$	cal/g-s	1.203E+10	1.195E+10	–1%	1.151E+10	–4%
	T_f(1 s)	K	3288	3290	+2 K	3311	+24 K
10,000	$t_{vol/mass}^{max}$ [a]	seconds	4.885E-04	5.021E-04	+3%	4.859E-04	–1%
	$\dot{q}_{vol}^{max}$	cal/cm^3-s	7.141E+09	6.980E+09	–2%	6.563E+09	–8%
	$\dot{q}_{mass}^{max}$	cal/g-s	3.674E+10	3.581E+10	–3%	3.455E+10	–6%
	T_f (1 s)	K	3338	3340	+2 K	3364	+26 K
20,000	$t_{vol/mass}^{max}$ [a]	seconds	2.653E-04	2.752E-04	+4%	2.672E-04	+1%
	$\dot{q}_{vol}^{max}$	cal/cm^3-s	2.501E+10	2.437E+10	–3%	2.281E+10	–9%
	$\dot{q}_{mass}^{max}$	cal/g-s	6.654E+10	6.436E+10	–3%	6.128!pE+10	–8%
	T_f(1 s)	K	3358	3361	+3 K	3387	+29 K

[a]To the number of significant digits necessary to establish whether the acceptance criteria were met, t_{vol}^{max} and t_{mass}^{max} were the same.

[b]The maximum appearing in the simulation produced by the full mechanism appears as a shoulder that does not have a local maximum when R1 and R2 were employed to produce the simulation.

Table 3 presents the results that were obtained for the pure 100-wt% NH_4ClO_4 HR simulations. It is observed that only $t_{vol/mass}^{max}$ values in simulations produced by R2 fail to meet the ±10%–±10 K acceptance criteria. We do not believe these discrepancies disqualify R2 for use in intended applications. Kotlar (2010) uniformly employed ±10% for variations in q_{vol}^{max}, q_{mass}^{max}, t_{vol}^{max}, and t_{mass}^{max} in his initial implementation of the TMM. Reported without precedent or explanation, this choice was presumably based on his intuition and/or observations he made in the course of developing the method. Given their effectiveness/efficacy in that application and all mechanism reduction efforts undertaken by our group since then, there has been no reason to critically examine the impact of relaxing the acceptance criterion for specific parameters. (There have, however, been cases in

which alternate criteria have been employed.) Indeed, given the number of variables involved, the complexity of their interactions, and the fundamental differences between a homogeneous reactor and combustion scenarios involving spatial dimensions, it would be quite difficult to quantify.

That said, observations regarding the difference in sensitivity to starting conditions of $t_{vol/mass}^{max}$ values in HR simulations and burning rate predictions based on the PREMIX/CYCLOPS framework indicate that the ±10% acceptance criterion for this parameter is probably more restrictive than it needs to be. For example, the difference in the $t_{vol/mass}^{max}$ values produced by the full mechanism for the AP system at 500 and 1,000 psia are 0.2071 and 0.0768 s, respectively—a 270% difference/increase. This difference is almost 4 times larger than the 70% difference in CYCLOPS-based estimates for AP's burning rates at these pressures that were produced with a reduced mechanism derived from an earlier version of the current full mechanism (McQuaid and Chen 2014).

Even more telling and relevant is the sensitivity of $t_{vol/mass}^{max}$ to the starting temperature of the simulation. For example, when the HR model is equipped with the full mechanism and the starting temperature of the 300 psia, the 100-wt% NH_4ClO_4 simulation is reduced 1 K (from 900 to 899 K), $t_{vol/mass}^{max}$ increases from 4.123×10^{-1} s to 4.389×10^{-1} s—a 6 % difference. This is notable because although the chemical compositions and starting temperature of the simulations that are compared for mechanism reduction are identical at $t = 0$ s, as already mentioned, the model HR system undergoes an initial "equilibration" step that significantly lowers the temperature. In the 100-wt% NH_4ClO_4 simulation at 300 psia, a drop of almost 300 K occurs in less than 1×10^{-9} s. Having no analog in the deflagration model results discussed in the next section, this aspect of the simulation was not considered in the mechanism screening process. Differences between results produced by the full and reduced mechanisms for the process at this early time are noticeable and undoubtedly contribute to the $t_{vol/mass}^{max}$ discrepancies.

One could, of course, attempt to address this issue by setting a tolerance on the temperature variation at some arbitrarily selected temporal point prior to the primary heat release event. However, since we do not believe that a 21% difference in the $t_{vol/mass}^{max}$ values produced by R2 and the full mechanism will result in as large a difference in the burning rate estimates produced by them, the imposition of such a criterion would likely have excluded potentially viable candidates. Moreover, even if the maximum difference in the burning rate estimates produced by the 2 approached 21%, from the standpoint of studying the pressure-dependent burning rates of AP-HTPB composite propellants, it would be acceptable as long as it varied slowly and consistently with pressure, preventing the introduction of artificial trends or the masking of real ones. Regardless, since the final arbiter of

the validity of relaxing this criterion will be how the results of a deflagration model equipped with R2 compare with experimental data, this issue is simply something about which potential users should be aware.

Table 4 shows the results that were obtained for the 80-20 NH_4ClO_4-R45M cases. It is observed that all the simulations produced by R1 meet the ±10%–±10 K acceptance criteria. Except for T_f values, that is also the case for the simulations produced by R2.

The T_f exceptions require explanation. As mentioned in Section 2, times on the order of 1 s were needed for the temperature difference between successive time points to approach 0, and that was the duration employed for the postreduction analysis. However, screening mechanisms on the basis of the T_f produced at such durations yielded candidates that generated simulations that did not well-mimic the T versus t trace near the major heat release feature. To address that issue, a much shorter time to compare "final" temperatures was specified, allowing deviations to exceed ±10 K at 1 s.

Considering this unexpected outcome, we noted that Kotlar (2010) used (again without precedent or explanation) ±200 K for the first published application of the TMM, and mechanisms produced with it subsequently demonstrated their ability to represent the combustion chemistry of interest. The employment of ±10 K for the reduction process in the current study stems from McQuaid (2013) finding that the use of a tighter tolerance for T_f variations produced fewer false positives. Moreover, the tighter tolerance did not significantly compromise the TMM's ability to produce mechanisms with targeted sizes. Given the successes achieved with mechanisms produced by Kotlar using ±200 K, we see no reason to be concerned about deviations in T_f of up to ±30 K in simulations in which the temperature rises more than 2,000 K.

As the final step of this stage of the vetting process, T versus t and $\dot{q}_{mass}$ versus t traces produced by R1, R2, and the full mechanism were plotted and compared. Results for the AP and 80-20 AP-HTPB systems at pressures from 300 to 22,000 psia (20–1,500 atm) were examined. Plots produced at 1,000 and 10,000 psia are representative and shown in Figs. 1 and 2. Overall, good agreement was observed between the HR simulation results produced by the 3 over the entire parameter space considered.

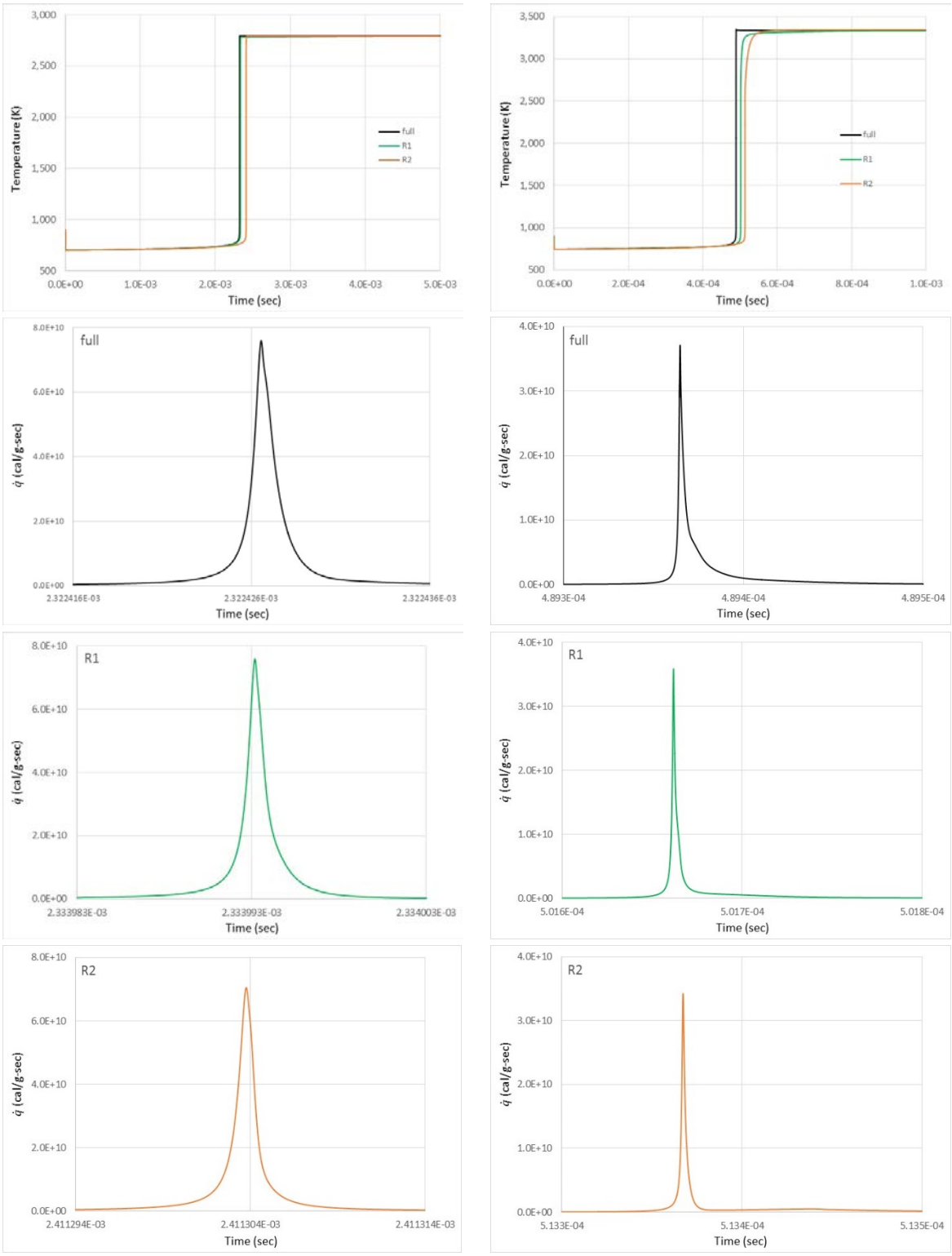

Fig. 2 Comparison of mass-specific heat release and temperature vs. time traces for CONP HR simulations produced with the full R1 and R2 mechanisms; 10,000 psia

4. Mechanism R2

Rate expressions for the elementary reaction steps comprising R2 are provided in Appendix A, which also provides information about the species involved. Appendix B provides data for calculating thermodynamic property estimates for species in the mechanism. Appendix C provides a look-up table for the molecular structure of species in the mechanism.

5. Burning Rate and Surface Temperature Predictions

5.1 Computational Methods

As a final check of the validity of R2 for intended applications, it was employed in a CYCLOPS model to compute burning rates for pure AP and 80-20 AP-HTPB. The CYCLOPS framework is described in detail elsewhere (Miller and Anderson 2000). Briefly, it involves running laminar, premixed flame simulations and finding values for the mass flux rate ($\dot{m}$) and temperature at the burner surface/condensed-phase-gas-phase interface (T_s or T^0) such that 2 conditions are satisfied. One is the conservation of energy (flux rate) at the condensed-phase-gas-phase interface.

$$\dot{m}\sum_i^N(Y_i^{-0}h_i^{+0} - Y_i^{-\infty}h_i^{-\infty}) - \lambda_g\left(\frac{dT}{dx}\right)^{+0} = 0, \quad (3)$$

where λ_g is the thermal conductivity of the gas mixture at the surface (in cal/cm-s-K), Y_i^{-0} are the mass fractions of the (N) nascent products (i) of the condensed phase's decomposition, h_i^{+0} are their enthalpies (in cal/g) at T_s, $Y_i^{-\infty}$ are the mass fractions of condensed-phase ingredients, and $h_i^{-\infty}$ are their enthalpies (in cal/g) at the starting bulk temperature ($T^{-\infty}$).

The second condition to be satisfied is the relationship between $\dot{m}$ and T_s. In all prior CYCLOPS-based studies, the relationship was established via a pyrolysis law.

$$\dot{m} = A_s exp(E_s/RT_s), \quad (4)$$

where A_s and E_s are constants (Miller and Anderson 2000). In the current study, however, the relationship between $\dot{m}$ and T_s was established through an evaporative/sublimative flux rate expression (Li et al. 1990; Miller 1997; Galwey and Brown 1999). For pure AP, the expression was

$$\dot{m}_{AP} - \sum_k(w_k/2\pi RT_s)^{\frac{1}{2}}(X_k^{-0}Aexp(-\Delta E/RT_s) - PX_k^{+0}) = 0, \quad (5)$$

Where X_k^{-0} and X_k^{+0} are, respectively, the mole fractions of the k^{th} nascent product on the condensed phase and gas-phase sides of the surface, P is the (total) pressure, A is the pre-exponential for the equilibrium vapor pressure, and ΔE is the effective

activation energy for dissociative sublimation. A (4.42×10^{13} dynes/cm^2) and ΔE (28,800 cal/mol) were specified on the basis of the dissociation pressures of AP that were measured by Inami et al. (1963).

To approximate the deflagration of an 80-20 AP-HTPB mixture, we employed the homogeneous representation of the gas phase enabled by PREMIX and required that the linear burning rate of HTPB ($r_b^{HTPB} = \dot{m}_{HTPB}/\rho_{HTPB}$) equal the linear burning rate of AP ($r_b^{AP} = \dot{m}_{AP}/\rho_{AP}$). With this constraint, it can be shown that

$$\dot{m}_{AP-HTPB} - (\rho_{AP-HTPB}/\rho_{AP})\dot{m}_{AP} = 0. \quad (6)$$

The laminar, premixed flame simulations were performed with a model employing the CHEMKIN III library of subroutines (Kee et al. 1985; Kee et al. 2002). Prior CYCLOPS models developed and employed by our group used CHEMKIN II subroutines. The change was made because simulation results produced by the latter for pure AP proved overly sensitive to the presence of reactions involving carbon-containing molecules. (They should have had no impact at all.) The calculation of $\lambda_g \left(\frac{dT}{dx}\right)^{+0}$ was also revised. Prior versions employed Newton forward differencing with a very limited number of (x,T) points to compute $\left(\frac{dT}{dx}\right)^{+0}$. In this study, numerical integration of

$$\lambda_g \left(\frac{dT}{dx}\right)^{+0} = \int_0^\infty q(x) exp\left[\frac{\dot{m}c_p x}{\lambda_g}\right] dx \quad (7)$$

was employed (Miller 1997). The volumetric enthalpy release [$q(x)$], mean gas-phase heat capacity (c_p), and λ_g values were computed via CHEMKIN III subroutines.

The condensed-phase properties of AP and HTPB that were employed for the calculations are shown in Table 5. The data employed to compute transport properties are given in Appendix D. Solutions for T_s and $\dot{m}_{AP/AP-HTPB}$ were found on a grid with T_s intervals of 0.01 K and $\dot{m}$ intervals of 0.001 g/cm^2-s. This resolution yielded residuals for Eq. 3 whose magnitudes were less than 0.01% of $\dot{m}\sum_i^N (Y_i^{-0} h_i^{+0} - Y_i^{-\infty} h_i^{-\infty})$, and residuals for Eqs. 5 or 7 whose magnitudes were less than 1% of $\dot{m}$.

Table 5 Condensed-phase properties of AP and HTPB employed to calculate burning rates

Material	ΔH_f (cal/g)	ρ (g/cm^3)
AP	–595	1.95
HTPB	–30	0.95
80-20 AP-HTPB	–482	1.75

5.2 Results

Table 6 presents the (T_s, $\dot{m}$) solutions that were found for pure AP burning at pressures from 300 to 20,000 psia. The burning rate estimates as a function of pressure are compared with measured values and previously computed estimates in Fig. 3. It is observed that the estimates computed with R2 are slightly higher than measured values at pressures from 300 to 2,000 psia, and they are approximately 50% higher than those estimated with a reduced mechanism obtained from a prior version of the AP only subset of the current full mechanism. Some of the latter difference is due to the difference in the manner in which $\lambda_g \left(\frac{dT}{dx}\right)^{+0}$ was computed. Given the limitations of the model and that trends are reproduced, we are satisfied with the agreement.

Table 6 The surface temperature, mass flux rate and burning rate of pure AP computed at various pressures by the R2-CYCLOPS model

Pressure (atm)	Pressure (psi)	T_s (K)	$\dot{m}$ (g/cm^2-s)	r_b (cm/s)
20	294	862	0.725	0.37
50	735	908	1.55	0.79
100	1,470	946	2.72	1.39
200	2,940	987	4.70	2.41
400	5,880	1,030	8.02	4.11
750	11,000	1,071	12.9	6.62
1,500	22,000	1,119	21.1	10.8

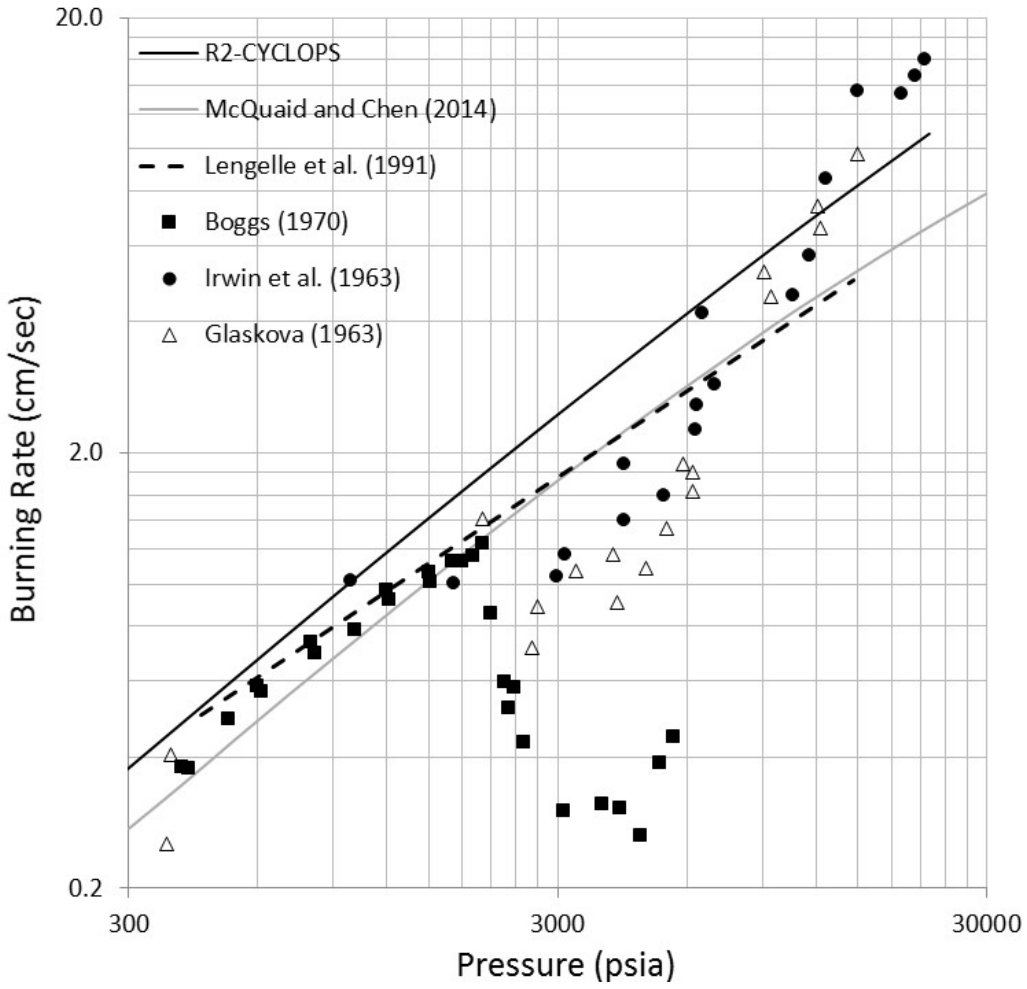

Fig. 3 Comparison of measured and computed burning rates for pure AP

The data in Table 6 also constitutes a basis for deriving a pyrolysis law. As shown in Fig. 4, a plot of $\ln(\dot{m})$ versus $1/T_s$ is nearly linear, and the fit to the data yields $A_s = 1.5 \times 10^6$ and $E_s = 25{,}200$ cal/mol. As shown in Table 7, these values fall in the middle of the range of values that have been proposed/employed by others. We also note that E_s is less than the value of ΔE (28,800 cal/mol) employed for Eq. 5. Figure 4 shows that they produce a relationship between $\dot{m}$ and T_s that is more similar to ones proposed by Beckstead et al. (1970) and Lengelle et al. (1991).

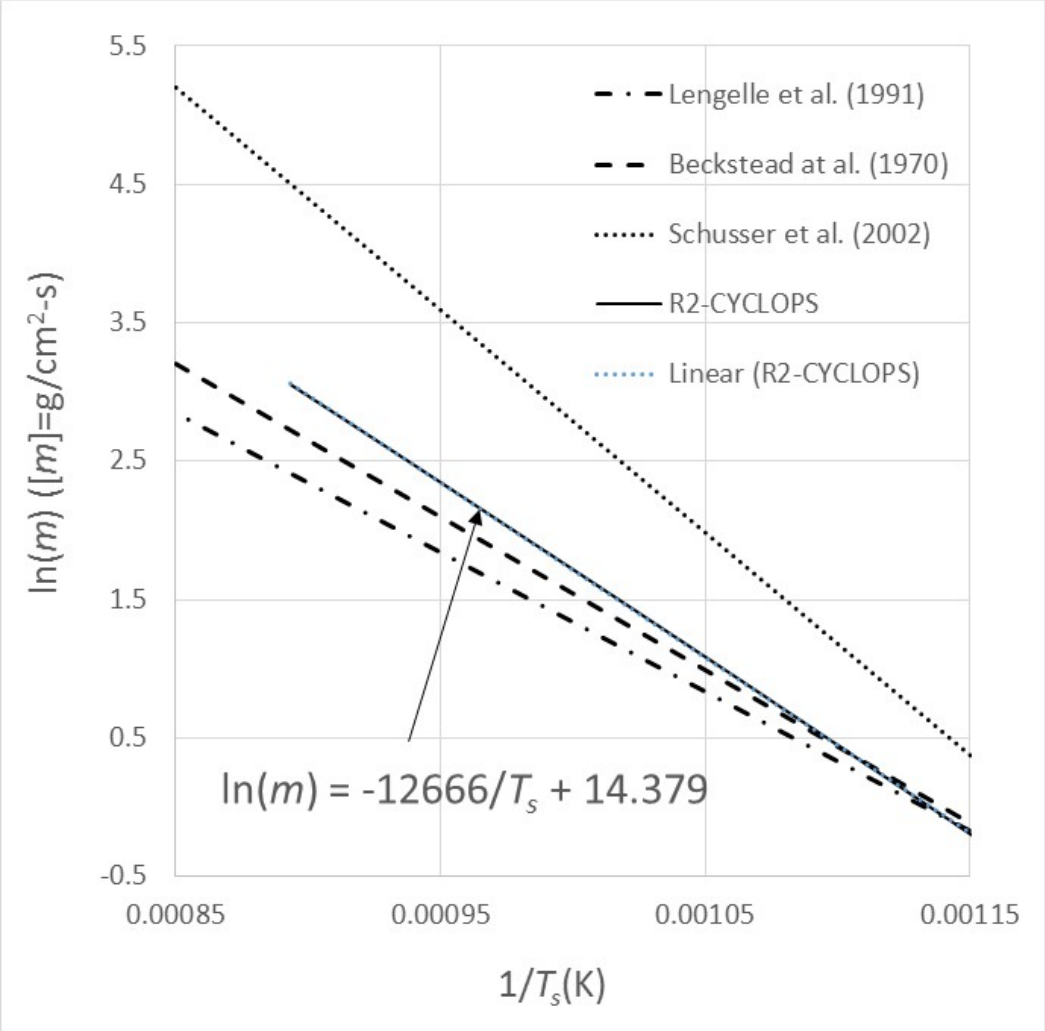

Fig. 4 Comparison of ln($\dot{m}$) vs. 1/Ts plots corresponding to different pyrolysis laws for pure AP

Table 7 Comparison of pyrolysis laws proposed for AP self-deflagration

Reference	A_s (g/cm^2-s)	E_s (cal/mol)
Lengelle et al. (1991)	9.6×10^4	20,000
Beckstead et al. (1970)	3.0×10^5	22,000
This work	1.8×10^6	25,200
Schusser et al. (2002)	1.6×10^8	32,000

Figure 5 presents a comparison of the R2-CYCLOPS-based burning rate estimates for the homogeneous 80-20 AP-HTPB mixture postulated in Section 2 with measured values for an 80-20 AP-HTPB mixture formulated with 5μ AP particles (Lengelle et al. 2002). (The mixture is probably as close to homogeneous as one can hope to attain.) While the agreement between traces is not compelling, the rates at a given pressure are within a factor of 2 of one another over the entire range

considered. Given the limitations of the (1-D, laminar) model—for example, for HTPB to regress (in nature) at the same linear rate as AP, the temperature of its surface must be much higher than that of AP's surface—the comparison is considered evidence that R2 will provide a reasonable representation of the gas-phase reaction kinetics of AP-HTPB systems in more detailed CFD models.

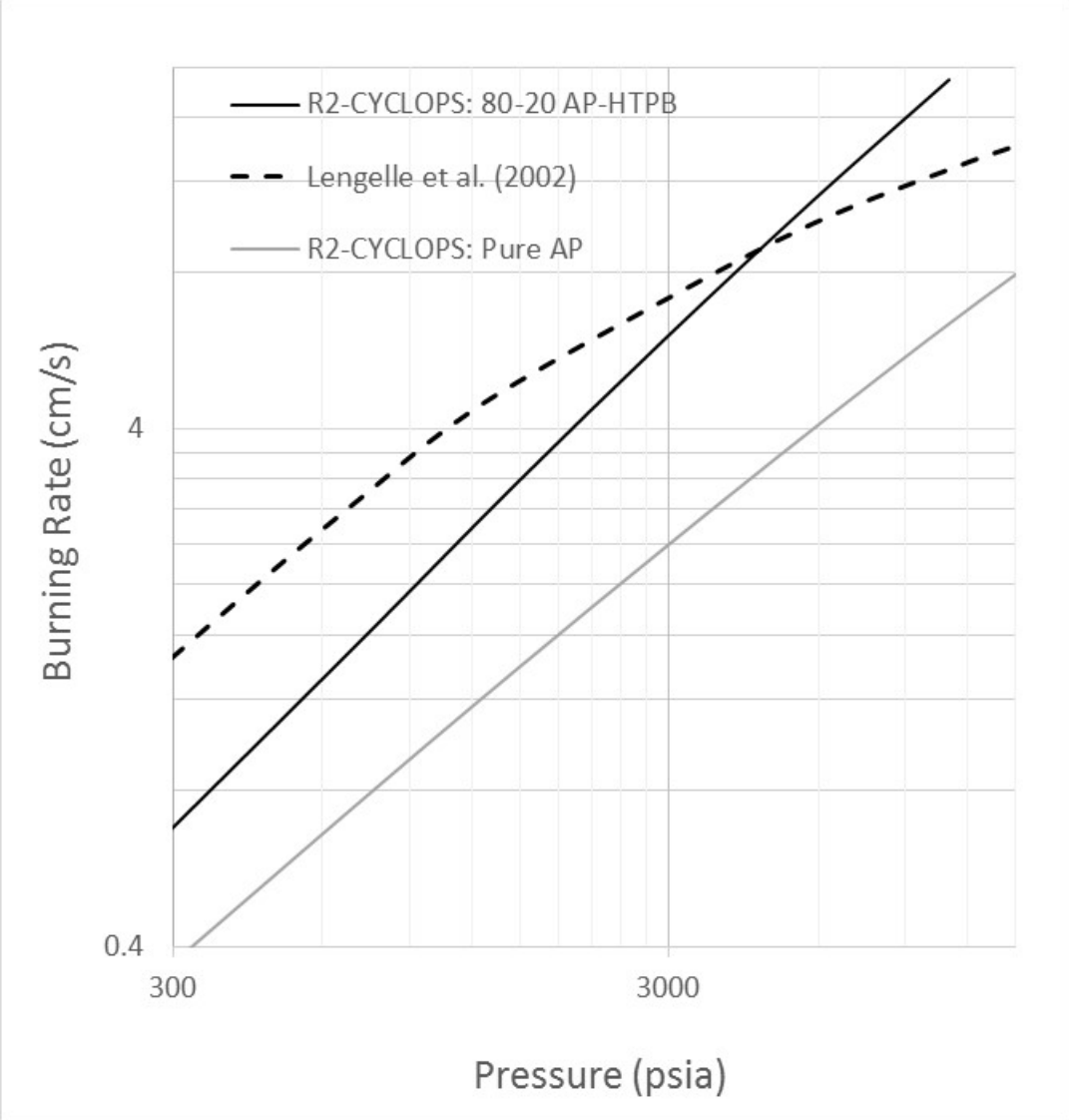

Fig. 5 Comparison of the pressure-dependent burning rates computed for a homogeneous 80-20 AP-HTPB mixture and measured values for an 80-20 AP-HTPB mixture formulated with 5μ AP particles

6. Additional Comments

Given the limited number of simulations that could be employed for the mechanism reduction process, mechanisms were not screened for their ability to mimic the oxidizer-free pyrolysis of HTPB. Based on the expectation that reactions involving oxidizers would dominate the latter stages of HTPB's decomposition, this decision left open the possibility that the reduction process would produce candidates that would not have a "hydrocarbon cracking submechanism" for representing the earliest stages of HTPB's decomposition. However, inspection of R2 indicates that it contains a set of reactions that could be considered such a submechanism. It includes a reaction in which R45M is "cracked" by collision with any species in the mechanism, and the daughters of that reaction have the potential to decompose via a sequence of steps that do not involve an oxidizer. Thus, the mechanism appears to have the potential to reasonably represent HTPB pyrolysis in CFD models of AP-HTPB composite propellant deflagration.

7. Summary and Conclusions

A (full) detailed, gas-phase, finite-rate chemical kinetics mechanism for representing the combustion chemistry associated AP-HTPB composite propellant deflagration was reduced to skeletal sets via the TMM. The full mechanism had 2,627 elementary reaction steps and involved 637 species. The primary objective of the effort was to produce a mechanism with ≤100 reactions and involving ≤100 species that could be employed as a submodel in the ARL CFD laminate framework. Results produced by trial mechanism–homogeneous reactor model combinations were the basis for eliminating reactions. Postreduction analyses were conducted to identify candidates with the best potential to mimic the full mechanism in a parameter space that is relevant to AP-HTPB composites burning at pressures from 300 to 20,000 psia. The candidate considered to be the best compromise between size and mimicking ability for this application had 100 reactions and involved 81 species. Coupled with the CYCLOPS framework, it produced estimates for the pressure-dependent burning rates of AP and a (hypothetical) homogeneous AP-HTPB mixture that were in reasonable agreement with measured burning rate data published in the open literature. All data comprising the mechanism are provided.

8. References

Atwood AI, Boggs TL, Curran O, Parr TP, Hanson-Parr DM, Price CF, Wiknich J. Burning rate of solid propellant ingredients. Part 1: pressure and initial temperature effects. Journal of Propulsion and Power. 1999;15:740–747.

Atwood AI, Ford KP, Wheeler CJ. High-pressure burning rate studies of solid rocket propellants. Progress in Propulsion Physics. 2013;4:3–14.

Beckstead, MW, Derr RL, Price CF. A model of composite solid-propellant combustion based on multiple flames. AIAA Journal. 1970;8:2200–2207.

Cai W, Thakre P, Yang V. A model of AP/HTPB composite propellant combustion in rocket motor environments. Combustion Science and Technology. 2008;180:2143–2169.

Chen C-C, McQuaid MJ. Thermochemical and kinetic studies of the pyrolysis of hydroxyl-terminated polybutadiene (HTPB). Presented at the 35th JANNAF Propellant and Explosives Characterization Subcommittee Meeting; 2009 Apr 14–17; Las Vegas, NM.

Chen C-C, McQuaid MJ. Modeling the deflagration of ammonium perchlorate at pressures from 300 to 30,000 psia. Part I: gas-phase, finite-rate, chemical kinetics mechanism development. Presented at the 46th JANNAF Combustion Subcommittee Meeting; 2014 Dec 8–11; Albuquerque, NM.

Chen C-C, McQuaid MJ. Thermochemical and kinetics modeling pertaining to AP-HTPB composite propellant combustion. Presented at the 39th JANNAF Propellant and Explosives Characterization Subcommittee Meeting; 2015 Dec 7–10; Salt Lake City, UT.

Chen C-C, McQuaid MJ. Thermochemistry and kinetics modeling of hydroxyl-terminated polybutadiene-red fuming nitric acid (HTPB-RFNA) systems. Presented at the 5th JANNAF Liquid Propulsion Subcommittee Meeting; 2010 May 3–7; Colorado Springs, CO.

Galwey AK., Brown ME. Thermal decomposition of ionic solids. Amsterdam (The Netherlands): Elsevier Science BV; 1999.

Gross ML, Beckstead MW. Steady-state combustion mechanism of ammonium perchlorate composite propellants. Journal of Propulsion and Power. 2011;27:1064–1078.

Gross ML, Hedman TD, Son SF, Jackson TL, Beckstead MW. Coupling micro and meso-scale combustion models of AP/HTPB propellants. Combustion and Flame. 2013;160:982–992.

Hedman TD, Reese DA, Cho KY, Groven LJ, Lucht RP, Son SF. An experimental study of the effects of catalysts on an ammonium perchlorate based composite propellant using 5 kHz PLIF. Combustion and Flame. 2012:159:1748–1758.

Inami SH, Rosser WA, Wise H. Dissociation pressure of ammonium perchlorate. Journal of Physical Chemistry. 1963;67:1077–1079.

Irwin OR, Salzman PK, Anderson WH. Deflagration characteristics of ammonium perchlorate at high pressures. Proceedings of the 9th Symposium (International) on Combustion; 1962 Sep 1; Ithaca NY; New York (NY): Elsevier; 1963. p. 358–364.

Kee RJ et al. Gas-phase kinetics. Chemkin Collection, Release 3.7. San Diego (CA): Reaction Design, Inc.; 2002.

Kee RJ, Rupley FM, Miller JA. Chemkin II: a Fortran chemical kinetics package for the analysis of gas-phase chemical kinetics. Albuquerque (NM): Sandia National Laboratories; 1989. Report No.: SAND89-8009.

Kee RJ, Grcar JF, Smooke MD, Miller JA. A FORTRAN program for modeling steady laminar one-dimensional premixed flames. Albequerque (NM): Sandia National Laboratories; 1985. Report No.: SAND85-2840.

Kotlar AJ. A general approach for the reduction of chemical reaction mechanisms I: methodology and application to MMH-RFNA. Presented at the 5th JANNAF Liquid Propulsion Subcommittee Meeting; 2010 May 3–7; Colorado Springs, CO.

Lengelle G, Duterque J-R, Godon J-C, Trubert, J-F. Solid propellant steady combustion-physical effects. In: Combustion of solid propellants. Brussels (Belgium): North Atlantic Treaty Organization; 1991. Report No.: AGARD-LS-180.

Lengelle G, Duterque J-R, Trubert J-F. Combustion of solid propellants. Brussels (Belgium): North Atlantic Treaty Organization; 2002. Report No.: RTO-EN-023.

Li SC, Williams FA, Margolis SB. Effects of two-phase flow in a model for nitramine deflagration. Combustion and Flame. 1990;80:329–349.

Li S, Petzold L. Software and algorithms for sensitivity analysis of large-scale differential algebraic systems. Journal of Computational and Applied Mathematics. 2000;125:131–145.

McQuaid MJ. The trial mechanism method for chemical kinetics mechanism reduction: an approach to developing mechanisms with wider ranges of applicability. Presented at the 7th JANNAF Liquid Propulsion Subcommittee Meeting; 2013 Apr 29–May 2; Colorado Springs, CO.

McQuaid MJ, Chen C-C. Modeling the deflagration of ammonium perchlorate at pressures from 300 to 30000 psia. Part II: considerations besides the gas-phase, finite-rate chemical kinetics mechanism. Presented at the 46th JANNAF Combustion Subcommittee Meeting; 2014 Dec 8–11; Albuquerque, NM.

Miller MS. Three-phase combustion modeling: frozen ozone, a prototype. Aberdeen Proving Ground (MD): Army Research Laboratory (US); 1997. Report No.: ARL-TR-1320.

Miller MS, Anderson WR. Energetic material combustion modeling with elementary gas-phase reactions: a practical approach. In: Solid propellant combustion chemistry: combustion and motor interior ballistics. Progress in Astronautics and Aeronautics, Vol. 185. Reston (VA): AIAA; 2000.

Nusca MJ. Computational fluid dynamics model of laminate AP/HTPB propellant strands: initial results for burn rate prediction. Presented at the 46th JANNAF Combustion Subcommittee Meeting; 2014 Dec 8–11; Albuquerque, NM.

Schusser M, Culick FEC, Cohen NS. Combustion response of ammonium perchlorate. AIAA Journal. 2002;40:722–730.

Surzhiknov ST, Krier H. Computational models of combustion of non-metallized heterogeneous propellant. High Temperature. 2003;41:95–128.

INTENTIONALLY LEFT BLANK.

Appendix A. Mechanism R2's Reactions, Rate Expressions, and Species Data

Table A-1 provides the elementary reaction steps comprising mechanism R2 and parameters for computing the rates (k) of the steps as a function of temperature (T) and pressure (P). Except for 2 reactions types that employ nonstandard methods for computing the rates of fall-off reactions, the reaction descriptions conform to standard Chemkin II notation and usage (Kee et al. 1989; references at end of Appendix A). The nonstandard methods for computing the rates for fall-off reactions are designated by the strings "T&H" (Tsang and Herron 1991) and "I*nn*", where *nn* is a number. For rates computed with T&H coefficients, "F_{cent}" (Kee et al. 1989) is calculated per

$$F_{cent} = a_0 + a_1 T + a_2 T^2,$$

where the polynomial's coefficients (a_i) are given in order after the T&H string. The second and/or third terms are zero if the coefficients are not provided.

For I*nn* fall-off reactions, reaction rates are calculated by logarithmically interpolating between rates at pressures that bound the one of interest (Cantera 2015). That is, given rate expressions,

$$k_1(T) = A_1 T^{b_1} exp(E_1/RT)$$

and

$$k_2(T) = A_2 T^{b_2} exp(E_2/RT)$$

at pressures P_1 and P_2, respectively, the rate at an intermediate pressure ($P_1 < P < P_2$) is computed per

$$\log k(T,P) = \log k_1(T) + (\log k_2(T) - \log k_1(T)) \frac{\log P - \log P_1}{\log P_2 - \log P_1}.$$

The coefficients following I*nn* in the tables correspond to A_i, b_i, E_i, and P_i (in atmospheres [atm]), respectively. We note that the numbers on the line that defines such reactions are dummy variables; they serve no function in computing rates. We also note that rate expressions applicable for pressures as low as 0.001 atm were developed. However, because R2 has been validated only for pressures as low as 20 atm, to reduce the computational expense of calculating the rates for such reactions, expressions for pressures less than 10 atm were omitted. That, in turn, resulted in certain sets in the table that do not exhibit fall-off behavior in the pressure range that is included. Such sets could be written more economically as a simple pressure-dependent form ("+M") with a single set of coefficients rather than in fall-off form ["(+M)"]. However, to prevent such expressions from being inadvertently adopted in this form for use in lower pressure applications, the fall-off form is specified.

The table also provides information about the species involved, including their elemental composition, molecular weight, and the temperature range over which

estimates for their thermodynamic properties have been computed. Data for computing the species' thermodynamic properties as a function of temperature are provided in Appendix B. Also, because Chemkin II limits the number of characters that can be employed to label a species to ≤16 characters, for many species it was not possible to assign a label or name that, within the context of the mechanism alone, could be reliably translated into a molecular structure. Appendix C provides a look-up table that performs that function.

Table A-1 Species and reaction rate expressions comprising mechanism R2

ELEMENTS CONSIDERED	ATOMIC WEIGHT
1. C	12.0112
2. H	1.00797
3. O	15.9994
4. N	14.0067
5. CL	35.4530

SPECIES CONSIDERED	PHASE	CHARGE	MOLECULAR WEIGHT	TEMPERATURE LOW	TEMPERATURE HIGH	ELEMENT COUNT C	H	O	N	CL
1. CHO	G	0	29.01852	300	5000	1	1	1	0	0
2. CH2O	G	0	30.02649	300	3500	1	2	1	0	0
3. CH3	G	0	15.03506	300	5000	1	3	0	0	0
4. CO	G	0	28.01055	300	5000	1	0	1	0	0
5. CO2	G	0	44.00995	300	5000	1	0	2	0	0
6. C2H2	G	0	26.03824	300	5000	2	2	0	0	0
7. C2H3	G	0	27.04621	300	5000	2	3	0	0	0
8. C*CCL*O	G	0	90.50976	300	5000	3	3	1	0	1
9. VCDJO	G	0	55.05676	300	5000	3	3	1	0	0
10. VCDO	G	0	56.06473	300	5000	3	4	1	0	0
11. CTCV	G	0	52.07648	300	5000	4	4	0	0	0
12. CDCCDCJ	G	0	53.08445	300	5000	4	5	0	0	0
13. CDCCDC	G	0	54.09242	300	5000	4	6	0	0	0
14. CCDOV	G	0	70.09182	300	5000	4	6	1	0	0
15. CDCCJC	G	0	55.10039	300	5000	4	7	0	0	0
16. VCOJC	G	0	71.09979	300	5000	4	7	1	0	0
17. CJVV	G	0	67.11154	300	5000	5	7	0	0	0
18. VVCOJ	G	0	83.11094	300	5000	5	7	1	0	0
19. CVV	G	0	68.11951	300	5000	5	8	0	0	0
20. CJCVC	G	0	69.12748	300	5000	5	9	0	0	0
21. CVCCVCL	G	0	144.64581	300	5000	8	13	0	0	1
22. VY6DE13J	G	0	105.16093	300	5000	8	9	0	0	0
23. VVVJV	G	0	105.16093	300	5000	8	9	0	0	0
24. VVVIV	G	0	106.16890	300	5000	8	10	0	0	0
25. VY6DE13	G	0	106.16890	300	5000	8	10	0	0	0
26. CVCZCVCJ	G	0	109.19281	300	5000	8	13	0	0	0
27. CVCCCOJV	G	0	125.19221	300	5000	8	13	1	0	0
28. CJCVCCVC	G	0	123.21990	300	5000	9	15	0	0	0
29. CVCCVCCOJ	G	0	139.21930	300	5000	9	15	1	0	0
30. BZBCCLV	G	0	198.73823	300	5000	12	19	0	0	1
31. BZBBJ	G	0	163.28523	300	5000	12	19	0	0	0
32. BZBCCOJV	G	0	179.28463	300	5000	12	19	1	0	0
33. BBBCJV	G	0	203.35056	300	5000	15	23	0	0	0
34. BBBCOJV	G	0	219.34996	300	5000	15	23	1	0	0
35. BBBJVIV	G	0	215.36172	300	5000	16	23	0	0	0
36. BBBVIV	G	0	216.36969	300	5000	16	24	0	0	0
37. R45MLSJ	G	0	307.93105	300	5000	20	32	0	0	1
38. R45MLPJ	G	0	307.93105	300	5000	20	32	0	0	1
39. R45M9J	G	0	271.47008	300	5000	20	31	0	0	0
40. R45M13J	G	0	271.47008	300	5000	20	31	0	0	0
41. R45M	G	0	272.47805	300	5000	20	32	0	0	0
42. CL	G	0	35.45300	300	5000	0	0	0	0	1

```
 43. HCL              G  0   36.46097   300   5000   0  1  0  0  1
 44. CLOH             G  0   52.46037   300   5000   0  1  1  0  1
 45. HOCLO            G  0   68.45977   300   4500   0  1  2  0  1
 46. HOOCL            G  0   68.45977   300   5000   0  1  2  0  1
 47. HOCLO2           G  0   84.45917   300   4500   0  1  3  0  1
 48. HCLO4            G  0  100.45857   300   4500   0  1  4  0  1
 49. NH4CLO4          G  0  117.48918   300   4500   0  4  4  1  1
 50. AP_NH3           G  0  134.51979   300   5000   0  7  4  2  1
 51. NOCL             G  0   65.45910   300   5000   0  0  1  1  1
 52. ONOCLO3          G  0  129.45670   300   4500   0  0  5  1  1
 53. CLO              G  0   51.45240   300   4500   0  0  1  0  1
 54. CLO2             G  0   67.45180   300   5000   0  0  2  0  1
 55. CLOO             G  0   67.45180   300   5000   0  0  2  0  1
 56. CLO3             G  0   83.45120   300   5000   0  0  3  0  1
 57. CL2              G  0   70.90600   300   5000   0  0  0  0  2
 58. H                G  0    1.00797   300   5000   0  1  0  0  0
 59. HNO              G  0   31.01407   300   5000   0  1  1  1  0
 60. HONO             G  0   47.01347   300   5000   0  1  2  1  0
 61. NNH              G  0   29.02137   250   4000   0  1  0  2  0
 62. HNJNO2           G  0   61.02017   300   5000   0  1  2  2  0
 63. HNOJNO2          G  0   77.01957   300   5000   0  1  3  2  0
 64. OH               G  0   17.00737   300   5000   0  1  1  0  0
 65. HO2              G  0   33.00677   300   5000   0  1  2  0  0
 66. H2               G  0    2.01594   300   5000   0  2  0  0  0
 67. NH2              G  0   16.02264   300   5000   0  2  0  1  0
 68. NH2O             G  0   32.02204   300   5000   0  2  1  1  0
 69. N2H2             G  0   30.02934   300   5000   0  2  0  2  0
 70. H2NNO2           G  0   62.02814   300   4500   0  2  2  2  0
 71. H2O              G  0   18.01534   300   5000   0  2  1  0  0
 72. NH3              G  0   17.03061   300   5000   0  3  0  1  0
 73. N2H3             G  0   31.03731   300   5000   0  3  0  2  0
 74. OJHNH3           G  0   34.03798   300   5000   0  4  1  1  0
 75. N2H4             G  0   32.04528   300   5000   0  4  0  2  0
 76. DINH3            G  0   34.06122   300   5000   0  6  0  2  0
 77. NO               G  0   30.00610   300   5000   0  0  1  1  0
 78. NO2              G  0   46.00550   300   5000   0  0  2  1  0
 79. N2               G  0   28.01340   300   5000   0  0  0  2  0
 80. O                G  0   15.99940   300   5000   0  0  1  0  0
 81. O2               G  0   31.99880   300   5000   0  0  2  0  0
-------------------------------------------------------------------------------

                                                (k = A T**b exp(-E/RT))     ref.
  REACTIONS CONSIDERED                            A        b         E

 1. R45M(+M)=BZBBJ+CVCZCVCJ(+M)                1.000E+00    0.00        0.0      a
      I05:   1.9800E+91 -2.3800E+01  7.9841E+04  1.0000E+01
      I24:   1.9800E+91 -2.3800E+01  7.9841E+04  2.0000E+03
 2. BZBBJ(+M)=CVCZCVCJ+CDCCDC(+M)              1.000E+00    0.00        0.0      b
      I05:   1.0300E+37 -7.8000E+00  3.6423E+04  1.0000E+01
      I24:   1.0300E+37 -7.8000E+00  3.6423E+04  2.0000E+03
 3. VVVIV=VY6DE13                              2.770E+13    0.00    45570.0      c
 4. VY6DE13+H=VY6DE13J+H2                      4.800E+08    1.50        0.0      d
 5. VY6DE13J=VVVJV                             1.429E+12    0.63    61604.0      g
 6. CTCV+CDCCDCJ=VVVJV                         3.160E+11    0.00     6000.0       e
 7. CTCV=C2H2+C2H2                             1.290E+15    0.00    82470.0      f
 8. C2H3+C2H2=CDCCDCJ                          1.260E+10    1.90     2110.0      h
 9. R45M+CL=R45M9J+HCL                         2.950E+14    0.00      180.0      j
10. R45M+CLO=R45M13J+CLOH                      3.443E+01    3.37     1728.4      k
11. R45M+CL=R45MLPJ                            1.780E+10    1.31    -1030.0      l
12. R45M+CL=R45MLSJ                            1.630E+14    0.00        0.0      m
13. R45MLSJ=BZBCCLV+CVCZCVCJ                   1.076E+12    0.44    19407.0      n
14. R45MLPJ=BZBBJ+CVCCVCL                      6.088E+11    0.51    18815.0      o
15. CVCZCVCJ+HO2=CVCCCOJV+OH                   9.640E+12    0.00        0.0      i
```

```
 16. VVCOJ=VCDO+C2H3                                2.306E+13    0.30    19668.0       g
 17. CDCCJC+CLO2(+M)=CCDOV+CLOH(+M)                 1.000E+00    0.00        0.0       p
       I05:   3.7800E+05  2.0600E+00 -1.6540E+03  1.0000E+01
       I06:   3.7600E+05  2.0600E+00 -1.6550E+03  2.5000E+01
       I07:   3.8600E+05  2.0600E+00 -1.6490E+03  5.0000E+01
       I08:   4.2700E+05  2.0500E+00 -1.6260E+03  7.5000E+01
       I09:   5.0800E+05  2.0200E+00 -1.5840E+03  1.0000E+02
       I10:   8.2300E+05  1.9600E+00 -1.4670E+03  1.5000E+02
       I11:   1.4200E+06  1.9000E+00 -1.3300E+03  2.0000E+02
       I12:   2.4600E+06  1.8300E+00 -1.1910E+03  2.5000E+02
       I13:   4.1300E+06  1.7600E+00 -1.0550E+03  3.0000E+02
       I14:   6.6900E+06  1.7000E+00 -9.2500E+02  3.5000E+02
       I15:   1.0400E+07  1.6500E+00 -8.0400E+02  4.0000E+02
       I16:   1.5600E+07  1.6000E+00 -6.9000E+02  4.5000E+02
       I17:   2.2600E+07  1.5600E+00 -5.8400E+02  5.0000E+02
       I18:   4.3000E+07  1.4800E+00 -3.9100E+02  6.0000E+02
       I19:   7.3800E+07  1.4100E+00 -2.2300E+02  7.0000E+02
       I20:   1.1600E+08  1.3600E+00 -7.4000E+01  8.0000E+02
       I21:   1.7000E+08  1.3100E+00  5.8000E+01  9.0000E+02
       I22:   2.3600E+08  1.2700E+00  1.7600E+02  1.0000E+03
       I23:   6.6200E+08  1.1600E+00  6.1800E+02  1.5000E+03
       I24:   1.0500E+09  1.1100E+00  9.0600E+02  2.0000E+03
 18. CDCCDC=C2H3+C2H3                               4.027E+19   -1.00    98150.0       q
 19. R45M9J=CVV+BBBCJV                              4.480E+10    0.56    21910.0       r
 20. CDCCJC+BBBVIV=R45M13J                          2.410E+10    2.48     6130.0       s
 21. BBBCJV+NO2(+M)=BBBCOJV+NO(+M)                  1.000E+00    0.00        0.0       t
       I05:   9.6100E+20 -2.2200E+00  1.1470E+04  1.0000E+01
       I06:   3.2500E+19 -1.7400E+00  1.1702E+04  2.5000E+01
       I07:   8.5000E+17 -1.2400E+00  1.1695E+04  5.0000E+01
       I08:   6.5400E+16 -9.0000E-01  1.1616E+04  7.5000E+01
       I09:   8.7600E+15 -6.3000E-01  1.1526E+04  1.0000E+02
       I10:   3.9500E+14 -2.1000E-01  1.1351E+04  1.5000E+02
       I11:   3.6300E+13  1.0000E-01  1.1192E+04  2.0000E+02
       I12:   5.1600E+12  3.6000E-01  1.1050E+04  2.5000E+02
       I13:   9.7900E+11  5.8000E-01  1.0922E+04  3.0000E+02
       I14:   2.3000E+11  7.7000E-01  1.0804E+04  3.5000E+02
       I15:   6.3500E+10  9.4000E-01  1.0697E+04  4.0000E+02
       I16:   1.9900E+10  1.0900E+00  1.0597E+04  4.5000E+02
       I17:   6.9100E+09  1.2300E+00  1.0504E+04  5.0000E+02
       I18:   1.0700E+09  1.4800E+00  1.0334E+04  6.0000E+02
       I19:   2.1100E+08  1.6900E+00  1.0183E+04  7.0000E+02
       I20:   5.0300E+07  1.8800E+00  1.0046E+04  8.0000E+02
       I21:   1.3900E+07  2.0400E+00  9.9210E+03  9.0000E+02
       I22:   4.3400E+06  2.2000E+00  9.8060E+03  1.0000E+03
       I23:   4.2800E+04  2.8000E+00  9.3340E+03  1.5000E+03
       I24:   1.4400E+03  3.2400E+00  8.9720E+03  2.0000E+03
 22. BBBCOJV=BZBBJ+VCDO                             4.287E+11    0.52     4984.3       u
 23. BZBBJ+NO2(+M)=BZBCCOJV+NO(+M)                  1.000E+00    0.00        0.0       t
       I05:   1.6600E+21 -2.2600E+00  1.2103E+04  1.0000E+01
       I06:   1.9200E+19 -1.6500E+00  1.2158E+04  2.5000E+01
       I07:   2.1600E+17 -1.0400E+00  1.2009E+04  5.0000E+01
       I08:   1.0200E+16 -6.3000E-01  1.1845E+04  7.5000E+01
       I09:   9.7000E+14 -3.2000E-01  1.1696E+04  1.0000E+02
       I10:   2.7400E+13  1.5000E-01  1.1438E+04  1.5000E+02
       I11:   1.8400E+12  5.1000E-01  1.1223E+04  2.0000E+02
       I12:   2.0500E+11  8.0000E-01  1.1038E+04  2.5000E+02
       I13:   3.2300E+10  1.0400E+00  1.0875E+04  3.0000E+02
       I14:   6.5000E+09  1.2500E+00  1.0729E+04  3.5000E+02
       I15:   1.5700E+09  1.4400E+00  1.0596E+04  4.0000E+02
       I16:   4.4100E+08  1.6000E+00  1.0475E+04  4.5000E+02
       I17:   1.3900E+08  1.7500E+00  1.0364E+04  5.0000E+02
       I18:   1.8100E+07  2.0200E+00  1.0163E+04  6.0000E+02
       I19:   3.1400E+06  2.2500E+00  9.9850E+03  7.0000E+02
```

```
      I20:   6.6800E+05  2.4500E+00  9.8260E+03  8.0000E+02
      I21:   1.6800E+05  2.6300E+00  9.6820E+03  9.0000E+02
      I22:   4.8100E+04  2.7900E+00  9.5500E+03  1.0000E+03
      I23:   3.4800E+02  3.4300E+00  9.0150E+03  1.5000E+03
      I24:   9.5300E+00  3.8900E+00  8.6110E+03  2.0000E+03
 24. BZBCCOJV=CJCVCCVC+VCDO                       3.451E+13    0.14    10168.0       v
 25. CJCVCCVC+NO2(+M)=CVCCVCCOJ+NO(+M)            1.000E+00    0.00        0.0       w
      I05:   2.6100E+13 -3.0000E-02  3.5000E+01  1.0000E+01
      I06:   2.8700E+13 -5.0000E-02  5.9000E+01  2.5000E+01
      I07:   4.2400E+13 -9.0000E-02  1.6200E+02  5.0000E+01
      I08:   6.8300E+13 -1.5000E-01  2.9400E+02  7.5000E+01
      I09:   1.0800E+14 -2.1000E-01  4.2500E+02  1.0000E+02
      I10:   2.3800E+14 -3.1000E-01  6.6400E+02  1.5000E+02
      I11:   4.4300E+14 -3.8000E-01  8.6600E+02  2.0000E+02
      I12:   7.2300E+14 -4.4000E-01  1.0370E+03  2.5000E+02
      I13:   1.0700E+15 -4.9000E-01  1.1830E+03  3.0000E+02
      I14:   1.4600E+15 -5.2000E-01  1.3090E+03  3.5000E+02
      I15:   1.8800E+15 -5.5000E-01  1.4190E+03  4.0000E+02
      I16:   2.3000E+15 -5.8000E-01  1.5170E+03  4.5000E+02
      I17:   2.7200E+15 -6.0000E-01  1.6030E+03  5.0000E+02
      I18:   3.4900E+15 -6.2000E-01  1.7500E+03  6.0000E+02
      I19:   4.0900E+15 -6.4000E-01  1.8710E+03  7.0000E+02
      I20:   4.5200E+15 -6.5000E-01  1.9720E+03  8.0000E+02
      I21:   4.7600E+15 -6.5000E-01  2.0570E+03  9.0000E+02
      I22:   4.8500E+15 -6.5000E-01  2.1300E+03  1.0000E+03
      I23:   3.9500E+15 -6.1000E-01  2.3780E+03  1.5000E+03
      I24:   2.5500E+15 -5.4000E-01  2.5150E+03  2.0000E+03
 26. CVCCVCCOJ=CVCZCVCJ+CH2O                      1.502E+11    0.54     9059.9       x
 27. CVCCCOJV=CJCVC+VCDO                          3.451E+13    0.14    10168.0       v
 28. BBBVIV+OH=BBBJVIV+H2O                        2.400E+06    2.00        0.0       d
 29. BBBJVIV=CVCZCVCJ+VVVIV                       4.019E+09    0.86    27888.0       y
 30. CO+C2H3=VCDJO                                1.510E+11    0.00     4810.0       z
 31. CJCVC+O=CVV+OH                               3.170E+12    0.03     -390.0      aa
 32. CVV+OH=CJVV+H2O                              3.600E+06    2.00        0.0       d
 33. CJVV+NO2(+M)=VVCOJ+NO(+M)                    1.000E+00    0.00        0.0       w
      I05:   2.6100E+13 -3.0000E-02  3.5000E+01  1.0000E+01
      I06:   2.8700E+13 -5.0000E-02  5.9000E+01  2.5000E+01
      I07:   4.2400E+13 -9.0000E-02  1.6200E+02  5.0000E+01
      I08:   6.8300E+13 -1.5000E-01  2.9400E+02  7.5000E+01
      I09:   1.0800E+14 -2.1000E-01  4.2500E+02  1.0000E+02
      I10:   2.3800E+14 -3.1000E-01  6.6400E+02  1.5000E+02
      I11:   4.4300E+14 -3.8000E-01  8.6600E+02  2.0000E+02
      I12:   7.2300E+14 -4.4000E-01  1.0370E+03  2.5000E+02
      I13:   1.0700E+15 -4.9000E-01  1.1830E+03  3.0000E+02
      I14:   1.4600E+15 -5.2000E-01  1.3090E+03  3.5000E+02
      I15:   1.8800E+15 -5.5000E-01  1.4190E+03  4.0000E+02
      I16:   2.3000E+15 -5.8000E-01  1.5170E+03  4.5000E+02
      I17:   2.7200E+15 -6.0000E-01  1.6030E+03  5.0000E+02
      I18:   3.4900E+15 -6.2000E-01  1.7500E+03  6.0000E+02
      I19:   4.0900E+15 -6.4000E-01  1.8710E+03  7.0000E+02
      I20:   4.5200E+15 -6.5000E-01  1.9720E+03  8.0000E+02
      I21:   4.7600E+15 -6.5000E-01  2.0570E+03  9.0000E+02
      I22:   4.8500E+15 -6.5000E-01  2.1300E+03  1.0000E+03
      I23:   3.9500E+15 -6.1000E-01  2.3780E+03  1.5000E+03
      I24:   2.5500E+15 -5.4000E-01  2.5150E+03  2.0000E+03
 34. VCDO+OH=VCDJO+H2O                            1.000E+13    0.00        0.0      bb
 35. VCOJC=VCDO+CH3                               1.453E+12    0.52    12665.0      cc
 36. VCOJC=H+CCDOV                                1.164E+10    1.09    12301.0      dd
 37. H+NO(+M)=HNO(+M)                             1.520E+15   -0.41        0.0      ee
     Low pressure limit:  0.40000E+21 -0.17500E+01  0.00000E+00
        N2O              Enhanced by    5.000E+00
        H2O              Enhanced by    5.000E+00
        N2               Enhanced by    1.000E+00
```

```
38. NO+OH(+M)=HONO(+M)                          1.988E+12   -0.05     -721.0      ee
    Low pressure limit:  0.50800E+24 -0.25100E+01 -0.67600E+02
    T&H VALUE:  0.62000E+00
       N2O              Enhanced by    5.000E+00
       H2O              Enhanced by    8.300E+00
       N2               Enhanced by    1.000E+00
39. HNO+NO2=HONO+NO                             4.420E+04    2.64     4042.0      ee
40. HNO+O=OH+NO                                 3.610E+13    0.00        0.0      ee
41. OH+H2=H2O+H                                 2.160E+08    1.50     3430.0      ee
42. NH2+NH2(+M)=N2H4(+M)                        1.000E+00    0.00        0.0      ee
      I05:   3.3100E+27 -4.5500E+00  3.9380E+03  1.0000E+01
      I06:   4.7100E+25 -3.9100E+00  3.5490E+03  2.5000E+01
      I07:   1.2700E+24 -3.3900E+00  3.1640E+03  5.0000E+01
      I08:   1.4200E+23 -3.0800E+00  2.9150E+03  7.5000E+01
      I09:   2.9900E+22 -2.8600E+00  2.7320E+03  1.0000E+02
      I10:   3.3600E+21 -2.5500E+00  2.4680E+03  1.5000E+02
      I11:   7.3300E+20 -2.3400E+00  2.2790E+03  2.0000E+02
      I12:   2.3000E+20 -2.1700E+00  2.1330E+03  2.5000E+02
      I13:   9.1100E+19 -2.0400E+00  2.0160E+03  3.0000E+02
      I14:   4.2200E+19 -1.9400E+00  1.9170E+03  3.5000E+02
      I15:   2.1900E+19 -1.8500E+00  1.8320E+03  4.0000E+02
      I16:   1.2400E+19 -1.7700E+00  1.7590E+03  4.5000E+02
      I17:   7.5500E+18 -1.7000E+00  1.6940E+03  5.0000E+02
      I18:   3.2500E+18 -1.5800E+00  1.5830E+03  6.0000E+02
      I19:   1.6200E+18 -1.4900E+00  1.4920E+03  7.0000E+02
      I20:   9.0500E+17 -1.4100E+00  1.4140E+03  8.0000E+02
      I21:   5.4700E+17 -1.3400E+00  1.3470E+03  9.0000E+02
      I22:   3.5300E+17 -1.2800E+00  1.2880E+03  1.0000E+03
      I23:   7.1400E+16 -1.0600E+00  1.0730E+03  1.5000E+03
      I24:   2.5300E+16 -9.1000E-01  9.3200E+02  2.0000E+03
43. N2H2+NH2=NH3+NNH                            1.000E+13    0.00     1000.0      ee
44. NH3+OH=NH2+H2O                              2.040E+06    2.04      566.0      ee
45. NH3(+M)=NH2+H(+M)                           6.600E+17    0.00    97280.0      ee
    Low pressure limit:  0.20400E+16  0.00000E+00  0.78780E+05
46. HNO+OH=NO+H2O                               1.295E+07    1.88     -958.0      ee
47. HNO+NH2=NH3+NO                              2.000E+13    0.00     1000.0      ee
48. NNH(+M)=N2+H(+M)                            4.100E+09    1.13     5186.0      ee
    Low pressure limit:  0.10000E+14  0.50000E+00  0.30600E+04
       N2O              Enhanced by    5.000E+00
       H2O              Enhanced by    9.000E+00
       N2               Enhanced by    1.000E+00
       O2               Enhanced by    8.200E-01
       NH3              Enhanced by    5.000E+00
49. HNO+O2=NO+HO2                               1.373E+01    3.56     7932.3      ff
50. HOOCL=HCL+O2                                8.602E+12    0.15       34.0      gg
51. HOOCL=HOCLO                                 2.659E+12    0.35       39.8      gg
52. OH+CLO2(+M)=HOCLO2(+M)                      1.000E+00    0.00        0.0      hh
      I05:   1.2600E+23 -3.9400E+00  5.4100E+02  1.0000E+01
      I06:   2.5800E+23 -3.9200E+00  6.7600E+02  2.5000E+01
      I07:   4.1200E+23 -3.8900E+00  8.0500E+02  5.0000E+01
      I08:   5.2500E+23 -3.8800E+00  8.9100E+02  7.5000E+01
      I09:   6.1500E+23 -3.8600E+00  9.5700E+02  1.0000E+02
      I10:   7.5000E+23 -3.8400E+00  1.0560E+03  1.5000E+02
      I11:   8.4600E+23 -3.8200E+00  1.1290E+03  2.0000E+02
      I12:   9.1600E+23 -3.8000E+00  1.1880E+03  2.5000E+02
      I13:   9.6800E+23 -3.7800E+00  1.2370E+03  3.0000E+02
      I14:   1.0100E+24 -3.7700E+00  1.2780E+03  3.5000E+02
      I15:   1.0300E+24 -3.7600E+00  1.3150E+03  4.0000E+02
      I16:   1.0500E+24 -3.7500E+00  1.3470E+03  4.5000E+02
      I17:   1.0700E+24 -3.7300E+00  1.3760E+03  5.0000E+02
      I18:   1.0800E+24 -3.7100E+00  1.4250E+03  6.0000E+02
      I19:   1.0800E+24 -3.6900E+00  1.4670E+03  7.0000E+02
      I20:   1.0700E+24 -3.6800E+00  1.5030E+03  8.0000E+02
```

```
      I21:   1.0500E+24 -3.6600E+00  1.5350E+03  9.0000E+02
      I22:   1.0300E+24 -3.6500E+00  1.5630E+03  1.0000E+03
      I23:   8.9900E+23 -3.5800E+00  1.6660E+03  1.5000E+03
      I24:   7.6700E+23 -3.5200E+00  1.7330E+03  2.0000E+03
 53. CLO+CLO=CL2+O2                              6.560E+10    0.66     3759.4      ii
 54. CLO+CLO=CL+CLOO                             8.190E+10    0.77     4307.8      ii
 55. CLO+CLO=CLO2+CL                             3.770E+13    0.01     5754.4      ii
 56. CLOO(+M)=CL+O2(+M)                          1.000E+00    0.00        0.0      jj
      I05:   6.2600E+09  8.0000E-02  2.5080E+03  1.0000E+01
      I06:   1.5600E+10  8.0000E-02  2.5120E+03  2.5000E+01
      I07:   3.1300E+10  8.0000E-02  2.5190E+03  5.0000E+01
      I08:   4.6700E+10  8.0000E-02  2.5260E+03  7.5000E+01
      I09:   6.2100E+10  9.0000E-02  2.5320E+03  1.0000E+02
      I10:   9.2300E+10  9.0000E-02  2.5430E+03  1.5000E+02
      I11:   1.2200E+11  9.0000E-02  2.5530E+03  2.0000E+02
      I12:   1.5100E+11  9.0000E-02  2.5630E+03  2.5000E+02
      I13:   1.7800E+11  9.0000E-02  2.5720E+03  3.0000E+02
      I14:   2.0600E+11  9.0000E-02  2.5810E+03  3.5000E+02
      I15:   2.3200E+11  9.0000E-02  2.5880E+03  4.0000E+02
      I16:   2.6800E+11  9.0000E-02  2.6040E+03  4.5000E+02
      I17:   2.8200E+11  1.0000E-01  2.6020E+03  5.0000E+02
      I18:   3.3200E+11  1.0000E-01  2.6160E+03  6.0000E+02
      I19:   3.7500E+11  1.0000E-01  2.6270E+03  7.0000E+02
      I20:   3.8500E+11  1.2000E-01  2.6260E+03  8.0000E+02
      I21:   4.6200E+11  1.1000E-01  2.6490E+03  9.0000E+02
      I22:   4.9700E+11  1.1000E-01  2.6570E+03  1.0000E+03
      I23:   6.8100E+11  1.2000E-01  2.6990E+03  1.5000E+03
      I24:   8.2900E+11  1.3000E-01  2.7300E+03  2.0000E+03
 57. CL+NH3=NH2+HCL                              3.248E+05    2.53     1322.0      kk
 58. CLO+NH3=NH2+CLOH                            1.130E+00    3.85     8631.5      ll
 59. CLO3+NH3=NH2+HOCLO2                         8.190E+09    1.01     4480.7      ll
 60. CLO+NH2=HCL+HNO                             2.830E+16   -1.08      256.3      mm
 61. CLO+NH2=CL+NH2O                             1.020E+15   -0.62       47.7      mm
 62. CLO3+NH2=CLO2+NH2O                          5.960E+15   -0.47       47.7      mm
 63. CLO+NH2O=CLOH+HNO                           2.000E+13    0.00        0.0      nn
 64. CLO2+NH2O=HOCLO+HNO                         2.000E+13    0.00     4210.0      oo
 65. CLO3+NH2O=HOCLO2+HNO                        2.000E+13    0.00        0.0      nn
 66. OH+CLO3(+M)=HO2+CLO2(+M)                    1.000E+00    0.00        0.0      pp
      I05:   1.2900E+14  9.0000E-02  3.9000E+01  1.0000E+01
      I24:   1.2900E+14  9.0000E-02  3.9000E+01  2.0000E+03
 67. CLO+NO(+M)=CL+NO2(+M)                       1.000E+00    0.00        0.0      qq
      I05:   1.3400E+13 -5.0000E-02  1.8000E+01  1.0000E+01
      I24:   1.3400E+13 -5.0000E-02  1.8000E+01  2.0000E+03
 68. CLO2+NO=CLO+NO2                             3.120E+11    0.39     -761.0      rr
 69. NOCL+H2O=HONO+HCL                           1.224E+11    0.23    11610.0      ss
 70. NOCL+NO=CLOO+N2                             1.700E+13    0.00     5625.0      bb
 71. HCL+CL=CL2+H                                1.500E+15    0.00    47550.0      tt
 72. CLOH+HNO=HCL+HONO                           3.480E+02    3.06     6068.3      uu
 73. HCLO4=CLO3+OH                               1.500E+17    0.00    52655.5      pp
 74. NH4CLO4=OJHNH3+CLO3                         1.500E+17    0.00    61560.0      vv
 75. OJHNH3=NH2+H2O                              1.091E+16    0.47     7036.9      ss
 76. OH+NH3=OJHNH3                               7.286E+10    0.64     -865.1      bb
 77. HCLO4+HONO=H2O+ONOCLO3                      3.226E+10    0.19       -1.0      ss
 78. ONOCLO3=CLO2+NO+O2                          2.458E+12    0.35    17353.0      ss
 79. NH2+NO=N2+OH+H                              8.990E+11    0.00        0.0      ee
 80. N2H3+N2H3=N2H4+N2H2                         1.200E+13    0.00        0.0      ww
 81. N2H4+NO2=N2H3+HONO                          5.603E+04    2.54     7787.0      ss
 82. N2H4+CLO3=N2H3+HOCLO2                       8.190E+09    1.01        0.0      bb
 83. NH2O+OH(+M)=NH2+HO2(+M)                     1.000E+00    0.00        0.0      xx
      I05:   2.0000E+24 -2.9900E+00  2.8296E+04  1.0000E+01
      I23:   2.0000E+24 -2.9900E+00  2.8296E+04  1.5000E+03
      I24:   1.9900E+24 -2.9900E+00  2.8296E+04  2.0000E+03
 84. NH2+NO2=NO+NH2O                             9.030E+11    0.03    -1512.1      yy
```

```
 85. NH2+NO2(+M)=H2NNO2(+M)                    1.000E+00    0.00        0.0      zz
       I05:   2.8900E+29 -5.6300E+00  3.5720E+03  1.0000E+01
       I06:   1.5000E+29 -5.4400E+00  3.5050E+03  2.5000E+01
       I07:   5.3800E+28 -5.2300E+00  3.4070E+03  5.0000E+01
       I08:   2.4700E+28 -5.0800E+00  3.3390E+03  7.5000E+01
       I09:   1.3100E+28 -4.9700E+00  3.2850E+03  1.0000E+02
       I10:   4.7200E+27 -4.7900E+00  3.1990E+03  1.5000E+02
       I11:   2.0700E+27 -4.6600E+00  3.1300E+03  2.0000E+02
       I12:   1.0300E+27 -4.5500E+00  3.0690E+03  2.5000E+02
       I13:   5.6200E+26 -4.4500E+00  3.0160E+03  3.0000E+02
       I14:   3.2700E+26 -4.3600E+00  2.9670E+03  3.5000E+02
       I15:   2.0000E+26 -4.2900E+00  2.9230E+03  4.0000E+02
       I16:   1.2800E+26 -4.2200E+00  2.8810E+03  4.5000E+02
       I17:   8.5000E+25 -4.1600E+00  2.8430E+03  5.0000E+02
       I18:   4.0700E+25 -4.0400E+00  2.7730E+03  6.0000E+02
       I19:   2.1300E+25 -3.9500E+00  2.7100E+03  7.0000E+02
       I20:   1.2000E+25 -3.8600E+00  2.6540E+03  8.0000E+02
       I21:   7.1300E+24 -3.7800E+00  2.6020E+03  9.0000E+02
       I22:   4.4400E+24 -3.7100E+00  2.5540E+03  1.0000E+03
       I23:   6.6700E+23 -3.4300E+00  2.3580E+03  1.5000E+03
       I24:   1.6500E+23 -3.2300E+00  2.2090E+03  2.0000E+03
 86. H2NNO2+NH2=HNJNO2+NH3                     4.820E+00    3.60      770.0     aaa
 87. HNJNO2+CLO2=HNOJNO2+CLO                   1.000E+13    0.00        0.0      bb
 88. HNOJNO2=HNO+NO2                           3.756E+13    0.31    12343.0      ss
 89. NH2O+NO2=HNO+HONO                         5.603E+04    2.54        0.0      ss
 90. CLO2+HNO=HOCLO+NO                         1.295E+01    3.24      651.5      ss
 91. HOCLO2+CL=CLO3+HCL                        3.550E-01    4.07     -340.0     bbb
 92. O+OH+M=HO2+M                              5.000E+16    0.00        0.0     ccc
 93. NH3+NH3=DINH3                             3.292E+07    1.82    -1391.5     ddd
 94. NH4CLO4+NH3=AP_NH3                        3.292E+07    1.82    -1391.5     ddd
 95. DINH3+HCLO4=AP_NH3                        3.292E+07    1.82    -1391.5     ddd
 96. CO+O2=CO2+O                               2.530E+12    0.00    47688.0      ee
 97. OH+CH2O<=>CHO+H2O                         3.430E+09    1.20     -447.0      ee
 98. C2H3+O2<=>CHO+CH2O                        4.580E+16   -1.40     1015.0      ee
 99. CHO+M=H+CO+M                              1.870E+17   -1.00    17000.0     fff
100. C*CCL*O+OH=VCDJO+CLOH                     3.500E+12    0.00    22810.0     eee

  NOTE:  A units mole-cm-sec-K, E units cal/mole
```

Notes

a. Estimate obtained via the Quantum-Rice-Ramsperger-Kassel (QRRK) method: 5-ethenyl-2,8-decadiene → 1-butene-3yl + 2,6-octadiene-1yl (Chen and McQuaid 2009).
b. Estimate obtained via QRRK: $CH_3CHCHCH_2CH_2CHCHC•H_2 \rightarrow CH_3CHCHC•H_2 + CH_2CHCHCH_2$.
c. Estimated from *trans*-$CH_2CHCHCHCHCH_2 \rightarrow$ 1,3-cyclohexadiene (Grimme et al. 1981).
d. From (Dean and Bozzelli 2000).
e. Estimate based on rate expression for $C_2H_2+C_2H_3 \rightarrow CH_2CHCHC•H$ found in Benson (1989).
f. From Kiefer et al. (1988).
g. Estimate based on transition state theory (TST). B1K-determined entropies were employed to calculate *A*. G3//B1K-based results were employed to calculate E_a.
h. From Weissman and Benson (1988).
i. From Tsang and Herron (1991).
j. Estimated from a rate expression for $C_3H_6 + Cl \rightarrow CH_2CHC•H_2 + HCl$ obtained from Pilgrim and Taatjes (1997).

k. Estimated from a TST-derived rate expression for ClO + *cis*-$CH_3CH(C_2H_3)CH_3 \rightarrow ClOH + CH_3C\bullet(C_2H_3)CH_3$. Density functional theory (DFT)-determined entropies were employed to calculate *A*. CBS-QB3-based results were employed to calculate E_a.

l. Estimated from a rate expression for $C_2H_4 + Cl \rightarrow C\bullet H_2CH_2Cl$ obtained from Knyazev et al. (1999).

m. Estimated from a rate expression for $C_3H_6 + Cl \rightarrow CH_3C\bullet HCH_2Cl$ obtained from Kaiser and Wallington (1996).

n. Estimated from a TST-derived rate expression for $CH_3CH(CHCH_2)CH_2C\bullet HCHClCH_3 \rightarrow CH_3CHCHC\bullet H_2 + CH_2CHCHClCH_3$. DFT-determined entropies were employed to calculate *A*. CBS-QB3-based results were employed to calculate E_a.

o. Estimated from a TST-derived rate expression for $CH_3CHCHCH_2CH(CH_3)C\bullet HCH_2Cl \rightarrow CH_3CHCHC\bullet H_2 + CH_3CHCHCH_2Cl$. DFT-determined entropies were employed to calculate *A*. CBS-QB3-based results were employed to calculate E_a.

p. Estimated via QRRK with a variational transition state theory (VTST)-derived rate expression for $CH_2CHC\bullet HCH_3 + ClO_2 \rightarrow CH_2CHCOClOHCH_3$ (5.94×10^4 $T^{2.36717}\exp(1723.4/RT)$ $cm^3\ mole^{-1}\ s^{-1}$) and a TST-derived rate expression for $CH_2CHCOClOHCH_3 \rightarrow CH_2CHCOCH_3 + ClOH$ (6.63×10^{11} $T^{0.21524}\exp(-8639.3/RT)$ s^{-1}).

q. From Curran et al. (2004).

r. Estimated based on a TST-derived rate expression for $CH_3CHCHCH(CHCH_2)CH_2C\bullet H_2 \rightarrow C_2HCH_2 + CH_3CHCHC\bullet HCHCH_2$. B1K-determined entropies were employed to calculate *A*. G3MP2//B1K-based results were employed to calculate E_a.

s. Estimated based on microscopic reversibility (MR) and a reverse rate expression for $CH_3 + C_2H_4 \rightarrow CH_3CHC\bullet H_2$ obtained from Curran (2006).

t. Estimated based on a QRRK-derived rate expression for $CH_2CHC\bullet H_2 + NO_2 \rightarrow CH_2CHCH_2O\bullet + NO$. Input included a VTST-derived rate expression for $CH_2CHC\bullet H_2 + NO_2 \rightarrow CH_2CHCH_2ONO$ (1.87×10^9 $T^{0.95983}\exp(-948/RT)$ $cm^3mole^{-1}s^{-1}$) and a rate expression for $CH_2CHCH_2ONO \rightarrow CH_2CHCH_2O\bullet + NO$ that was estimated based on MR and a reverse rate expression for $CH_3O + NO \rightarrow CH_3ONO$ obtained from Caralp et al. (1998).

u. Estimated based on a TST-derived rate expression for $CH_2CHCO\bullet HCH_2CHCH_2 \rightarrow CH_2CHCHO + CH_2CHC\bullet H_2$. B1K-determined entropies were employed to calculate *A*. G3//B1K-based results were employed to calculate E_a.

v. Estimated based on a TST-derived rate expression for $CH_2CHCO\bullet HCH_2CH_2CH_3 \rightarrow CH_2CHCHO + CH_3CH_2C\bullet H_2$. B1K-determined entropies were employed to calculate *A*. G3//B1K-based results were employed to calculate E_a.

w. Estimated based on a QRRK-derived rate expression for $CH_3C\bullet H_2 + NO_2 \rightarrow CH_3CH_2O\bullet + NO$. Input included a rate expression for $CH_3C\bullet H_2 + NO_2 \rightarrow CH_3CH_2ONO$ that was estimated to be 2.03×10^{13} $cm^3mol^{-1}s^{-1}$ and a rate expression for $CH_3CH_2ONO \rightarrow CH_3CH_2O\bullet + NO$ that was estimated based on MR and a reverse rate expression for $CH_3O + NO \rightarrow CH_3ONO$ obtained from Caralp et al. (1998).

x. Estimated based on a TST-derived rate expression for $CH_2CHCH_2CH_2O\bullet \rightarrow CH_2CHC\bullet H_2 + CH_2O$. B1K-determined entropies were employed to calculate *A*. G3//B1K-based results were employed to calculate E_a.

y. Estimated based on a TST-derived rate expression for $CH_3CHCHCH_2CH_2CHCHC\bullet H_2 \rightarrow CH_3CHCHC\bullet H_2 + CH_2CHCHCH_2$. B1K-determined entropies were employed to calculate *A*. G3//B1K-based results were employed to calculate E_a.

z. From Tsang and Hampson (1986).
aa. Estimated from a rate expression for $C_2H_5 + O \rightarrow C_2H_4 + OH$ obtained from Harding et al. (2005).
bb. Estimated in this study.
cc. Estimated from a TST-derived rate expression for CH2CHCH2CHO•CH3 → CH2CHCHO + CH3. B1K-determined entropies were employed to calculate A. G3//B1K-based results were employed to calculate Ea.
dd. Estimated based on a TST-derived rate expression for CH2CHCH2CHO•CH3 → CH2CHCOCH3 + H. B1K-determined entropies were employed to calculate A. G3//B1K-based results were employed to calculate Ea.
ee. From Anderson et al. (2011).
ff. Estimated via TST with an H-atom tunneling correction. DFT-determined entropies were employed to calculate A. G4- and CBS-QB3-based results were employed to calculate Ea.
gg. From Xu et al. (2003)
hh. Estimated via QRRK with input obtained from Xu et al. (2003).
ii. From Zhu and Lin (2003a).
jj. Estimated via QRRK with input obtained from Zhu and Lin (2003b).
kk. From Monge-Palacios and Espinosa-Garcia (2010).
ll. From Xu and Lin (2007)
mm. From Zhu and Lin (2007).
nn. Estimated from results obtained for Cl + NH2O → HCl + HNO.
oo. A was estimated based on results obtained for Cl + NH2O → HCl + HNO. G4-based results were employed to calculate Ea.
pp. Estimated via QRRK with input obtained from Zhu and Lin (2001).
qq. From Zhu and Lin (2004).
rr. Estimated based on a rate expression for ClO + NO → Cl + NO2 obtained from Zhu and Lin (2004).
ss. Estimated based on TST with an H-atom tunneling correction. DFT-determined entropies were employed to calculate A. G4-based results were employed to calculate Ea.
tt. NIST (Manion et al. 2013) Two-parameter fit to rates for HCl + Cl → Cl2 + H.
uu. From Xu and Lin (2010).
vv. A was estimated based on the rate expression for HClO4 → ClO3 + OH. G4-based results were employed to calculate Ea.
ww. From Sun et al. (2009).
xx. Estimated via QRRK with a rate expression for NH2O + OH → NH2OOH that was estimated to be 1.81 x 1013 cm3mole-1s-1. Input included a rate expression for NH2OOH → NH2 + HO2 that was based on MR and reverse rate expression for NH2 + HO2 → NH2OOH that was obtained from Bozzelli and Dean (1989).
yy. From Klippenstein et al. (2013).
zz. Estimated via QRRK with input obtained from Klippenstein et al. (2013).
aaa. Estimated based on a rate expression for $N_2H_4 + NH_2 \rightarrow NH_3 + N_2H_3$ obtained from Li and Zhang (2006).
bbb. Estimated based on a rate expression for HOCl + Cl → HCl + ClO obtained from Wang et al. (2003).
ccc. From Burke et al. (2010).

ddd. Estimated based on a rate expression for NH3 + HClO4 → NH4ClO4 obtained from Zhu and Lin (2008).
eee. From Ho et al. (1995) and Procaccini et al. (2000).
fff. From Timonen et al. (1987).

References

Anderson WR, Meagher NE, Vanderhoff JA. Dark zones of solid propellant flames: critically assessed datasets, quantitative model comparison, and detailed chemical analysis. Combustion and Flame. 2011;158:1228-1244.

Benson, SW. The mechanism of the reversible reaction: $2C_2H_2 \leftrightarrow$ vinyl acetylene and the pyrolysis of butadiene. International Journal of Chemical Kinetics. 1989;21:233–243.

Bozzelli JW, Dean AM. Energized complex quantum Rice-Ramsperger-Kassel analysis on reactions of amidogen with hydroperoxo, oxygen and oxygen atoms. Journal of Physical Chemistry. 1989;3:1058–1065.

Burke MP, Chaos M, Dryer, FL, Ju Y. Negative pressure dependence of mass burning rates of $H_2/CO/O_2$/diluent flames at low flame temperatures. Combustion and Flame. 2010;157:618–631.

Cantera [accessed 2015]. www.cantera.org.

Caralp F, Rayez M-T, Forst W, Gomez N, Delcroix B, Fittschen C, Devolder P. Kinetic and mechanistic study of the pressure and temperature dependence of the reaction CH_3O + NO. Journal of the Chemical Society: Faraday Transactions. 1998;94:3321–3330.

Chen C-C, McQuaid MJ. Thermochemical and kinetic studies of the pyrolysis of hydroxyl-terminated polybutadiene (HTPB). Presented at the 35th JANNAF Propellant and Explosives Characterization Subcommittee Meeting; 2009 Apr 14–17; Las Vegas, NM.

Curran HJ, Pitz W J, Westbrook CK. NC7_2b mechanism, UCRL-WEB-204236, [accessed Oct 2014 . http://www.cms.llnl.gov/combustion/.

Curran HJ. Rate constant estimation for C-1 to C-4 alkyl and alkoxyl radical decomposition. International Journal of Chemical Kinetics. 2006;38:250–275.

Dean AM, Bozzelli JW. Combustion chemistry of nitrogen. In: Gardiner WC Jr., editor. Gas-phase combustion chemistry. New York (NY): Springer-Verlag; 2000.

Grimme W, Schumachers L, Roth WR, Breuckmann R. anti-[4 + 4]-dicyclopentadien. Chemische Berichte. 1981;114:3197–3470.

Harding LB, Klippenstein SJ, Georgievskii Y. Reactions of oxygen atoms with hydrocarbon radicals: a priori kinetic predictions for the CH_3+O, C_2H_5+O, and C_2H_3+O reactions. Proceedings of the Combustion Institute. 2005;30:985–993.

Ho W, Booty MR, Magee RS, Bozzelli JW. Analysis and optimization of chlorocarbon incineration through the use of a detailed reaction mechanism. Industrial & Engineering Chemistry Research. 1995;34:4185–4192.

Kaiser EW, Wallington TJ. Pressure dependence of the reaction Cl + C_3H_6. Journal of Physical Chemistry. 1996;100:9788–9793.

Kee RJ, Rupley FM, Miller JA. Chemkin II: A Fortran chemical kinetics package for the analysis of gas-phase chemical kinetics. Albuquerque (NM): Sandia National Laboratories;1989. Report No.: SAND89-8009.

Kiefer JH, Mitchell KI, Kern RD, Yong, JN. Unimolecular dissociation of vinylacetylene: a molecular reaction. Journal of Physical Chemistry. 1988;92:677–685.

Klippenstein SJ, Harding LB, Glarborg P, Gao Y, Hu H, Marshall P. Rate constant and branching fraction for the NH2 + NO2 reaction. Journal of Physical Chemistry A. 2013;117:9011–9022.

Knyazev VD, Kalinovski IJ, Slagle IR. Kinetics of the $CH_2CH_2Cl = C_2H_4$+ Cl reaction. Journal of Physical Chemistry A. 1999;103:3216–3221.

Li QS, Zhang X. Direct dynamics study on the hydrogen abstraction reactions $N_2H_4 + R \rightarrow N_2H_3 + RH$ ($R=NH_2,CH_3$). Journal of Chemical Physics. 2006;125:064304.

Manion JA et al. NIST chemical kinetics database, NIST standard reference database 17, version 7.0 (web version), release 1.6.8, data version 2013.03. Gaithersburg (MD): National Institute of Standards and Technology; 2013.

Monge-Palacios M, Espinosa-Garcia J. Reaction-path dynamics calculations of the Cl + NH_3 hydrogen abstraction reaction: the role of the intermediate complexes. Journal of Physical Chemistry A. 2010;114:4418–4426.

Pilgrim JS, Taatjes CA. Infrared absorption probing of the Cl + C_3H_6 reaction: rate coefficients for HCl production between 290 and 800 K. Journal of Physical Chemistry A. 1997;101:5776–5782.

Procaccini C, Bozzelli JW, Longwell JP, Smith KA, Sarofim AF. Presence of chlorine radicals and formation of molecular chlorine in the post-flame region of chlorocarbon combustion. Environmental Science and Technology. 2000;34:4565–4570.

Sun H, Catoire L, Law CK. Thermal decomposition of monomethylhydrazine: shock tube experiments and kinetic modeling. International Journal of Chemical Kinetics. 2009;41:176–186.

Timonen RS, Ratajczak E, Gutman D, Wagner AF. The addition and dissociation reaction H + CO = HCO.2: experimental studies and comparison with theory. Journal of Physical Chemistry. 1987;91:5325–5332.

Tsang W, Hampson RF. Chemical kinetic data base for combustion chemistry: I. methane and related compounds. Journal of Physical and Chemical Reference Data. 1986;15:1087–1279.

Tsang W, Herron JT. Chemical kinetic data base for propellant combustion: I. reactions involving NO, NO_2, HNO, HNO_2, HCN and N_2O. Journal of Physical and Chemical Reference Data. 1991;20:609–623.

Wang L, Liu J-y, Li Z-s, Huang X-r, Sun C-c. Theoretical study and rate constant calculation of the Cl + HOCl and H + HOCl reactions. Journal of Physical Chemistry A. 2003;107:4921–4928.

Weissman MA, Benson SW. Rate parameters for the reactions of C_2H_3 and C_4H_5 with H_2 and C_2H_2. Journal of Physical Chemistry. 1988;92:4080–4084.

Xu ZF, Lin MC. Computational studies on the kinetics and mechanisms for NH_3 reactions with ClOx (x = 0 - 4) radicals. Journal of Physical Chemistry A. 2007;111:584–590.

Xu ZF, Lin MC. Computational studies on metathetical and redox processes of HOCl in gas phase: III. its self-reaction and interactions with HNOx (x = 1-3). Journal of Physical Chemistry A. 2010;114:5320–5326.

Xu ZF, Zhu RS, Lin MC. Ab initio studies of ClOx reactions: III. kinetics and mechanism for the OH + OClO reaction. Journal of Physical Chemistry A. 2003;107:1040–1049.

Zhu RS, Lin MC. Ab initio study of ammonium perchlorate combustion initiation processes: unimolecular decomposition of perchloric acid and the related OH + ClO_3 reaction. PhysChemComm. 2001;25:1–5.

Zhu RS, Lin MC. Ab initio studies of ClOx reactions: IV. kinetics and mechanism for the self-reaction of ClO radicals. Journal of Chemical Physics. 2003;118:4094–4106.

Zhu RS, Lin MC. Ab initio studies of ClOx reactions: VIII. isomerization and decomposition of ClOO and related bimolecular processes. Journal of Chemical Physics. 2003;119:2075–2082.

Zhu RS, Lin MC. Ab initio studies of ClOx reactions: X. prediction of the rate constants of ClO + NO for the forward and reverse processes. ChemPhysChem. 2004;5:1864–1870.

Zhu RS, Lin MC. Ab initio study of the ClO + NH_2 reaction: prediction of the total rate constant and product branching ratios. Journal of Physical Chemistry A. 2007;111:3977–8393.

Zhu R, Lin MC. Mechanism and kinetics for ammonium perchlorate sublimation: a first-principles study. Journal of Physical Chemistry C. 2008;112:14481–14485.

INTENTIONALLY LEFT BLANK.

Appendix B. Coefficients for Calculating Thermodynamic Property Estimates for Species in Mechanism R2

Coefficients for computing estimates for the heat capacity [$c_p(T)$], enthalpy $H(T)$, and entropy [$S(T)$] of species in mechanism R2 are given in Table B-1. The data conform to standard Chemkin II formatting rules.[1] Because the CHEMKIN II framework limits the labels for species to 16 or fewer characters, for many species it was not possible to assign labels that can be unambiguously translated into a molecular structure. A look-up table that performs that function is provided in Appendix C.

Table B-1 Coefficients for calculating thermodynamic property estimates for species in mechanism R2

```
THERMO
   300.000  1500.000  5000.000
CHO                 ESTC   1H   1O   1    0G   300.000  5000.000 1367.000    01
 3.69472521E+00 3.18594296E-03-1.08841412E-06 1.68761454E-10-9.77966305E-15    2
 3.82240388E+03 4.69145660E+00 3.53025733E+00 1.88364239E-03 1.78452098E-06    3
-1.72919680E-09 3.98120351E-13 4.08521632E+03 6.23492345E+00                   4
CH2O              L 8/88H   2C   1O   1   00G   300.000  3500.000  1000.000    1
 1.76069008E+00 9.20000082E-03-4.42258813E-06 1.00641212E-09-8.83855640E-14    2
-1.39958323E+04 1.36563230E+01 4.79372315E+00-9.90833369E-03 3.73220008E-05    3
-3.79285261E-08 1.31772652E-11-1.43089567E+04 6.02812900E-01 1.00197170E+04    4
CH3               121286C   1H   3          G  0300.00   5000.00  1000.00     1
 0.02844052E+02 0.06137974E-01-0.02230345E-04 0.03785161E-08-0.02452159E-12    2
 0.01643781E+06 0.05452697E+02 0.02430443E+02 0.01112410E+00-0.01680220E-03    3
 0.01621829E-06-0.05864953E-10 0.01642378E+06 0.06789794E+02                   4
CO                121286C   1O   1          G  0300.00   5000.00  1000.00     1
 0.03025078E+02 0.01442689E-01-0.05630828E-05 0.01018581E-08-0.06910952E-13    2
-0.01426835E+06 0.06108218E+02 0.03262452E+02 0.01511941E-01-0.03881755E-04    3
 0.05581944E-07-0.02474951E-10-0.01431054E+06 0.04848897E+02                   4
CO2               121286C   1O   2          G  0300.00   5000.00  1000.00     1
 0.04453623E+02 0.03140169E-01-0.01278411E-04 0.02393997E-08-0.01669033E-12    2
-0.04896696E+06-0.09553959E+01 0.02275725E+02 0.09922072E-01-0.01040911E-03    3
 0.06866687E-07-0.02117280E-10-0.04837314E+06 0.01018849E+03                   4
C2H2              121386C   2H   2          G  0300.00   5000.00  1000.00     1
 0.04436770E+02 0.05376039E-01-0.01912817E-04 0.03286379E-08-0.02156710E-12    2
 0.02566766E+06-0.02800338E+02 0.02013562E+02 0.01519045E+00-0.01616319E-03    3
 0.09078992E-07-0.01912746E-10 0.02612444E+06 0.08805378E+02                   4
C2H3               12787C   2H   3          G  0300.00   5000.00  1000.00     1
 0.05933468E+02 0.04017746E-01-0.03966740E-05-0.01441267E-08 0.02378644E-12    2
 0.03185435E+06-0.08530313E+02 0.02459276E+02 0.07371476E-01 0.02109873E-04    3
-0.01321642E-07-0.01184784E-10 0.03335225E+06 0.01155620E+03                   4
C*CCL*O    6/19/97      C   3H   3O   1CL  1G   300.000  5000.000 1398.000    11
 1.14618122E+01 8.45109469E-03-2.90073879E-06 4.51447285E-10-2.62376318E-14    2
-2.42075137E+04-3.15944471E+01 2.31820028E+00 3.25587682E-02-2.78476237E-05    3
 1.23566507E-08-2.20723840E-12-2.13016608E+04 1.65465029E+01                   4
VCDJO     VCDJO_G3MP2_G3C   3H   3N   0O   1G   300.000  5000.000 1403.000    01
 8.76612341E+00 7.77928992E-03-2.49026790E-06 3.69252827E-10-2.07329959E-14    2
 7.79908556E+03-1.86491247E+01 2.10804239E+00 2.79698291E-02-2.62572868E-05    3
 1.29707093E-08-2.52092364E-12 9.65945852E+03 1.54835048E+01                   4
VCDO      VCDO_G3MP2_G3_C   3H   4N   0O   1G   300.000  5000.000 1392.000    01
 9.39918255E+00 1.01168249E-02-3.36959545E-06 5.14172946E-10-2.94835284E-14    2
-1.23594302E+04-2.47300373E+01 1.13047846E+00 2.92269879E-02-1.99974542E-05    3
 6.98466320E-09-9.79237748E-13-9.49490843E+03 1.97052158E+01                   4
```

[1] Kee RJ, Rupley FM, Miller JA. Chemkin II: A Fortran chemical kinetics package for the analysis of gas-phase chemical kinetics. Albuquerque (NM): Sandia National Laboratories;1989. Report No.: SAND89-8009.

```
CTCV      10/ 2/ 9      C   4H   4    0    0G   300.000  5000.000 1392.000    11
 1.12367761E+01 8.82364166E-03-3.07153201E-06 4.82681345E-10-2.82467653E-14    2
 2.92566868E+04-3.57336366E+01-2.99968136E-02 3.79242319E-02-3.25061220E-05    3
 1.42322491E-08-2.50323956E-12 3.28915781E+04 2.37912229E+01                   4
CDCCDCJ   CDCCDC_BK1+VINC   4H   5N   0O   0G   300.000  5000.000 1416.000    11
 1.13163593E+01 1.05404088E-02-3.49684912E-06 5.31843737E-10-3.04168815E-14    2
 3.77210212E+04-3.59442045E+01-2.23870963E+00 4.90400762E-02-4.56067276E-05    3
 2.13268736E-08-3.90283982E-12 4.16788073E+04 3.43185309E+01                   4
CDCCDC    CDCCDC_BK1.outC   4H   6N   0O   0G   300.000  5000.000 1415.000    11
 1.14271967E+01 1.29584495E-02-4.32307232E-06 6.59997414E-10-3.78462012E-14    2
 7.61440843E+03-3.84271070E+01-3.16530048E+00 5.26021422E-02-4.58866872E-05    3
 2.04344500E-08-3.60678263E-12 1.20575132E+04 3.78560375E+01                   4
CCDOV      9/20/ 9 THERMC   4H   6O   1    0G   300.000  5000.000 1377.000    21
 1.11282775E+01 1.59830571E-02-5.50607262E-06 8.58928005E-10-4.99984492E-14    2
-1.91689528E+04-3.24493094E+01 2.54576818E+00 2.94344471E-02-9.79064273E-06    3
-1.18684688E-09 9.30612708E-13-1.55068149E+04 1.60207425E+01                   4
CDCCJC    CDCCJC_BK1.outC   4H   7N   0O   0G   300.000  5000.000 1398.000    11
 1.01661141E+01 1.66497350E-02-5.60871682E-06 8.61680146E-10-4.96213850E-14    2
 1.06328953E+04-2.95337476E+01 1.50306344E-02 3.93239957E-02-2.48355443E-05    3
 8.25242412E-09-1.13970812E-12 1.42842549E+04 2.53881891E+01                   4
VCOJC     VCOJC_G3MP2_BKC   4H   7N   0O   1G   300.000  5000.000 1399.000    21
 1.26649548E+01 1.66701855E-02-5.62013651E-06 8.63922637E-10-4.97707528E-14    2
 1.02185455E+03-3.98930857E+01 1.00184346E+00 4.48313850E-02-3.21345956E-05    3
 1.24303453E-08-2.01042644E-12 5.00471004E+03 2.24592295E+01                   4
CJVV      CVV+C*CC*CCJ  C   5H   7N   0O   0G   300.000  5000.000 1400.000    21
 1.42616569E+01 1.59801497E-02-5.53201590E-06 8.65987714E-10-5.05377999E-14    2
 1.60483386E+04-5.14843851E+01-3.16510508E+00 5.81304216E-02-4.45756765E-05    3
 1.73181146E-08-2.70632680E-12 2.19065453E+04 4.15138582E+01                   4
VVCOJ     10/ 1/ 9 THERMC   5H   7O   1    0G   300.000  5000.000 1392.000    21
 1.61589892E+01 1.62628904E-02-5.49172543E-06 8.45860293E-10-4.88215034E-14    2
 1.04839262E+04-5.77280669E+01-4.66489790E-01 5.87881110E-02-4.79917613E-05    3
 2.04451484E-08-3.53334092E-12 1.58832224E+04 3.02451397E+01                   4
CVV       CVV_BK1.out   C   5H   8N   0O   0G   300.000  5000.000 1418.000    21
 1.38617204E+01 1.79152384E-02-5.99017788E-06 9.15801819E-10-5.25631321E-14    2
 2.33368455E+03-4.95140504E+01-2.58120389E+00 5.94956538E-02-4.62659544E-05    3
 1.85895355E-08-3.00239718E-12 7.64306740E+03 3.75273996E+01                   4
CJCVC     E_CJCVC_BK1.ouC   5H   9N   0O   0G   300.000  5000.000 1392.000    31
 1.26311714E+01 2.11968230E-02-7.14277909E-06 1.09751772E-09-6.32060952E-14    2
 1.47076618E+04-3.78871255E+01 2.63277613E+00 4.03212036E-02-1.95983508E-05    3
 4.02307329E-09-1.64144521E-13 1.86551000E+04 1.73968930E+01                   4
CVCCVCL    GA           C   8H  13    0CL  1G   300.000  5000.000 1394.000    51
 2.46598556E+01 3.10368744E-02-1.06566786E-05 1.65880732E-09-9.64168975E-14    2
-1.22695766E+04-9.68688306E+01-2.27668100E+00 9.60910608E-02-7.18927947E-05    3
 2.83739559E-08-4.63021828E-12-3.08132966E+03 4.71199220E+01                   4
VY6DE13J  10/ 1/ 9 THERMC   8H   9    0    0G   300.000  5000.000 1403.000    01
 2.16368750E+01 2.26941806E-02-7.71538060E-06 1.19318832E-09-6.90455495E-14    2
 1.96559386E+04-9.23086148E+01-7.49360260E+00 1.04258843E-01-9.67113872E-05    3
 4.54442654E-08-8.41355134E-12 2.83839413E+04 5.92838342E+01                   4
VVVJV     10/ 1/ 9      C   8H   9    0    0G   300.000  5000.000 1397.000    21
 2.26301412E+01 2.15222007E-02-7.42096286E-06 1.15824454E-09-6.74430236E-14    2
 4.14479674E+04-9.30067034E+01-2.38964234E+00 9.38131205E-02-9.00665415E-05    3
 4.44147356E-08-8.62995317E-12 4.88904389E+04 3.66858499E+01                   4
VVVIV      9/24/ 9 THERMC   8H  10    0    0G   300.000  5000.000 1400.000    31
 2.35223129E+01 2.26391306E-02-7.75078445E-06 1.20391708E-09-6.98662618E-14    2
 1.48137893E+04-9.98670223E+01-4.64836883E+00 1.06599512E-01-1.05830849E-04    3
 5.31747258E-08-1.04157863E-11 2.28979384E+04 4.51819888E+01                   4
VY6DE13   10/ 1/ 9 THERMC   8H  10    0    0G   300.000  5000.000 1399.000    11
 2.17179798E+01 2.52472190E-02-8.70462989E-06 1.35877977E-09-7.91356320E-14    2
 8.67540826E+03-9.49443753E+01-7.26461799E+00 1.02109939E-01-8.86409603E-05    3
 3.96451662E-08-7.10924565E-12 1.78323550E+04 5.74743892E+01                   4
```

```
CVCZCVCJ  ZCVCECVCJ_BK1.C   8H  13N   0O   0G   300.000  5000.000 1399.000    41
 2.06302783E+01 3.16096497E-02-1.06933406E-05 1.64774759E-09-9.50929829E-14    2
 1.00684682E+04-7.75910549E+01-8.73966644E-01 7.96074824E-02-5.09359894E-05    3
 1.67164961E-08-2.22051441E-12 1.77593242E+04 3.86897908E+01                   4
CVCCCOJV   9/14/ 9 THERMC   8H  13O   1    0G   300.000  5000.000 1394.000    61
 2.49450780E+01 3.06606517E-02-1.05906573E-05 1.65509800E-09-9.64664386E-14    2
-1.69588863E+03-1.00312800E+02-2.85259996E+00 9.81220359E-02-7.45350560E-05    3
 2.97846865E-08-4.91192074E-12 7.76060818E+03 4.81750535E+01                   4
CJCVCCVC  CJCVCCVC_G3MP2C   9H  15N   0O   0G   300.000  5000.000 1393.000    61
 2.31262384E+01 3.61193184E-02-1.22113663E-05 1.88070319E-09-1.08492875E-13    2
 1.28522075E+04-8.62856416E+01 3.22491856E+00 7.65942108E-02-4.17019077E-05    3
 1.07581676E-08-9.72030195E-13 2.04256370E+04 2.28293599E+01                   4
CVCCVCCOJ  9/14/ 9 THERMC   9H  15O   1    0G   300.000  5000.000 1393.000    61
 2.68751263E+01 3.59826535E-02-1.22801111E-05 1.90393513E-09-1.10365105E-13    2
-5.09466492E+03-1.07916456E+02-3.13932770E+00 1.06607204E-01-7.62737417E-05    3
 2.85244844E-08-4.39829458E-12 5.29230351E+03 5.31236804E+01                   4
BZBCCLV    GA           C  12H  19    0CL  1G   300.000  5000.000 1394.000    81
 3.69272158E+01 4.46080955E-02-1.52938580E-05 2.37832056E-09-1.38146309E-13    2
-1.37613553E+04-1.58089386E+02-2.45844070E+00 1.40525666E-01-1.06376675E-04    3
 4.24358334E-08-6.98080128E-12-4.21163780E+02 5.21382628E+01                   4
BZBBJ      9/ 3/ 9 THERMC  12H  19    0    0G   300.000  5000.000 1394.000    71
 3.34182780E+01 4.53424770E-02-1.55200912E-05 2.41081354E-09-1.39924170E-13    2
 7.80723881E+03-1.41886056E+02-5.06283930E+00 1.37664846E-01-1.01521140E-04    3
 3.94256080E-08-6.32734200E-12 2.09736691E+04 6.39958354E+01                   4
BZBCCOJV   9/14/ 9 THERMC  12H  19O   1    0G   300.000  5000.000 1396.000    81
 3.58261146E+01 4.55360593E-02-1.56116413E-05 2.42762726E-09-1.41003538E-13    2
-3.26823346E+03-1.51933464E+02-4.82372585E+00 1.45587197E-01-1.11815564E-04    3
 4.52844427E-08-7.54806140E-12 1.03936648E+04 6.46655280E+01                   4
BBBCJV     9/ 8/ 9 THERMC  15H  23    0    0G   300.000  5000.000 1392.000    91
 4.21443837E+01 5.41028924E-02-1.83763736E-05 2.84055456E-09-1.64330500E-13    2
 9.64655606E+03-1.84798280E+02-5.41422303E+00 1.67056317E-01-1.21466085E-04    3
 4.58947967E-08-7.10170752E-12 2.59398952E+04 6.99026162E+01                   4
BBBCOJV    9/14/ 9      C  15H  23O   1    0G   300.000  5000.000 1395.000    91
 4.69273361E+01 5.08221788E-02-1.68954273E-05 2.57613604E-09-1.47682896E-13    2
-2.24128532E+03-2.06447571E+02-8.70352630E+00 1.93263406E-01-1.57828780E-04    3
 6.62988458E-08-1.11863416E-11 1.56309957E+04 8.75685214E+01                   4
BBBJVIV    9/23/ 9      C  16H  23    0    0G   300.000  5000.000 1397.000    81
 4.53398889E+01 5.42797942E-02-1.84165219E-05 2.84443257E-09-1.64453049E-13    2
 1.30903627E+04-2.02489154E+02-8.49422360E+00 1.92592763E-01-1.57233014E-04    3
 6.70603758E-08-1.15989944E-11 3.05087870E+04 8.21449680E+01                   4
BBBVIV     9/21/ 9 THERMC  16H  24    0    0G   300.000  5000.000 1395.000    91
 4.55309829E+01 5.56991305E-02-1.87927585E-05 2.89184539E-09-1.66770818E-13    2
 1.01854566E+03-2.01769691E+02-6.74779653E+00 1.88529451E-01-1.50543355E-04    3
 6.31731157E-08-1.08020559E-11 1.80887113E+04 7.51796905E+01                   4
R45MLSJ    GA           C  20H  32    0CL  1G   300.000  5000.000 1401.000    91
 5.81197997E+01 7.70298838E-02-2.59074195E-05 3.97708196E-09-2.28937919E-13    2
-1.08787019E+04-2.56271126E+02-7.75715090E+00 2.41490030E-01-1.85182312E-04    3
 7.48361961E-08-1.23663228E-11 1.08639815E+04 9.36459570E+01                   4
R45MLPJ    GA           C  20H  32    0CL  1G   300.000  5000.000 1400.000    91
 5.69292555E+01 7.76902385E-02-2.60568680E-05 3.99218566E-09-2.29482359E-13    2
-8.31259134E+03-2.47362318E+02-5.16097675E+00 2.32449762E-01-1.76191351E-04    3
 7.11121480E-08-1.18094929E-11 1.22664116E+04 8.26309623E+01                   4
R45M9J     9/14/ 9      C  20H  31    0    0G   300.000  5000.000 1397.000    91
 5.41954130E+01 7.60118675E-02-2.57157280E-05 3.96336250E-09-2.28782260E-13    2
 4.14284906E+03-2.42354496E+02-8.49772505E+00 2.28437547E-01-1.69268628E-04    3
 6.61645785E-08-1.06448625E-11 2.53051226E+04 9.22049786E+01                   4
R45M13J    9/14/ 9      C  20H  31    0    0G   300.000  5000.000 1397.000    91
 5.37073656E+01 7.64348507E-02-2.58637427E-05 3.98670412E-09-2.30151543E-13    2
 3.16363536E+03-2.39605966E+02-7.68140544E+00 2.23309632E-01-1.61418268E-04    3
 6.13997057E-08-9.62322323E-12 2.41220366E+04 8.88343536E+01                   4
```

```
R45M       9/ 3/ 9 THERMC  20H  32    0    0G   300.000  5000.000 1398.000    91
 5.42506578E+01 7.80424196E-02-2.63133838E-05 4.04604518E-09-2.33170301E-13    2
-1.27596349E+04-2.41212500E+02-8.28123127E+00 2.30655861E-01-1.70734012E-04    3
 6.69535506E-08-1.08218149E-11 8.29386157E+03 9.22860686E+01                   4
CL                 42189CL  1               G  0300.00   5000.00  1000.00      1
 0.02920237E+02-0.03597985E-02 0.01294294E-05-0.02162776E-09 0.01376517E-13    2
 0.01371338E+06 0.03262690E+02 0.02381577E+02 0.08891079E-02 0.04070476E-05    3
-0.02168943E-07 0.01160827E-10 0.01383999E+06 0.06021818E+02                   4
HCL                42189CL  1H   1          G  0300.00   5000.00  1000.00      1
 0.02755335E+02 0.01473581E-01-0.04971254E-05 0.08108658E-09-0.05072063E-13    2
-0.01191806E+06 0.06515116E+02 0.03338534E+02 0.01268207E-01-0.03666917E-04    3
 0.04703992E-07-0.01836011E-10-0.01213151E+06 0.03193555E+02                   4
CLOH      CLOH_G4.out   CL  1H   1N   0O   1G   300.000  5000.000 1425.000    01
 4.43819619E+00 1.90159701E-03-5.96736743E-07 8.70883543E-11-4.82905289E-15    2
-1.06618194E+04 2.38417393E+00 3.06962329E+00 6.26906774E-03-5.88061081E-06    3
 2.91620508E-09-5.65510463E-13-1.03069268E+04 9.31295623E+00                   4
HOCLO         RE-FIT   0CL  1O   2H   1    0G   300.000  4500.000 1000.00    0 1
 7.74227524E+00 1.14072335E-03-2.31095854E-07 3.98547731E-12 2.08972960E-15    2
-1.45044632E+02-1.21025028E+01 2.33550334E+00 2.18212549E-02-3.31039046E-05    3
 2.53351029E-08-7.72997812E-12 1.09269873E+03 1.44913387E+01                   4
HOOCL     HOOCL_G4_500 0CL  1O   2H   1    0G   300.000  5000.000 1000.00     01
 7.30200672D+00 1.61192543D-03-2.79065802D-07-8.62328785D-12 4.19722528D-15    2
-3.95942041D+03-1.06943293D+01 2.04355669D+00 2.22975388D-02-3.53793621D-05    3
 2.91689375D-08-9.50023046D-12-2.73718311D+03 1.51445456D+01                   4
HOCLO2        RE-FIT   0CL  1O   3H   1    0G   300.000  4500.000 1000.00    0 1
 9.81116772E+00 1.69027515E-03-3.38129098E-07 6.20168803E-12 2.95764614E-15    2
-4.73636133E+03-2.22311096E+01 2.01147413E+00 3.20615619E-02-4.95894456E-05    3
 3.85937575E-08-1.19048773E-11-2.97052759E+03 1.60160770E+01                   4
HCLO4         RE-FIT   0CL  1O   4H   1    0G   300.000  4500.000 1000.00     01
 1.15020361E+01 2.52951309E-03-4.60134316E-07-1.21791145E-11 6.90475085E-15    2
-4.85042920E+03-3.10284100E+01 7.20484078E-01 4.04154994E-02-5.86621500E-05    3
 4.58601157E-08-1.47678085E-11-2.12432935E+03 2.30658550E+01                   4
NH4CLO4       RE-FIT   0CL  1O   4N   1H   4G   300.000  4500.000 1000.00     01
 1.83178654E+01 5.24443667E-03-8.23817004E-07-5.82090626E-11 1.65948001E-14    2
-2.06336816E+04-6.58034286E+01 8.88326347E-01 6.68014288E-02-9.49331952E-05    3
 7.32077581E-08-2.32674401E-11-1.62725293E+04 2.14922791E+01                   4
AP_NH3    COMP_IRCF_TS_HCL  1H   7N   2O   4G   300.000  5000.000 1398.000    01
 1.82581064E+01 1.71061668E-02-5.61372775E-06 8.47432147E-10-4.82092675E-14    2
-3.36788636E+04-6.80892417E+01 4.65325755E+00 5.32755888E-02-4.33406078E-05    3
 1.89695077E-08-3.38376847E-12-2.93871425E+04 3.43034349E+00                   4
NOCL      CLNO_G4.out   CL  1N   1O   1    0G   300.000  5000.000 1378.000    01
 5.53178844E+00 1.30076647E-03-4.61294870E-07 7.33729585E-11-4.32941107E-15    2
 4.44818405E+03-8.99851231E-01 4.13186473E+00 4.51656794E-03-3.33281748E-06    3
 1.26992097E-09-2.01164271E-13 4.94565126E+03 6.64809180E+00                   4
ONOCLO3     RE-FIT     0CL  1N   1O   5    0G   300.000  4500.000 1000.00     01
 1.67813644E+01 1.11842831E-03-3.38921268E-07 3.39122758E-11-1.90400672E-16    2
 1.27917109E+04-5.48439751E+01 3.10192537E+00 4.29901779E-02-5.48648932E-05    3
 3.81883822E-08-1.18209947E-11 1.65361426E+04 1.52785330E+01                   4
CLO        RE-FIT      0CL  1O   1    0    0G   300.000  4500.000 1000.00    0 1
 4.23923159D+00 1.93449261D-04-4.25335251D-08 7.09551287D-13 4.32926348D-16    2
 1.07950146D+04 2.15147686D+00 2.92077899D+00 4.09045443D-03-4.49257323D-06    3
 2.48358267D-09-6.10953779D-13 1.11498711D+04 8.91226196D+00                   4
CLO2      CLO2_G4.out   CL  1H   0N   0O   2G   300.000  5000.000 1408.000    01
 6.13221573E+00 8.17125271E-04-3.00956329E-07 4.90756142E-11-2.94593271E-15    2
 9.74125871E+03-4.93151693E+00 2.78920691E+00 1.03639661E-02-1.07452184E-05    3
 5.19247877E-09-9.57201985E-13 1.07053068E+04 1.23677689E+01                   4
CLOO      CLOO_G4.out   CL  1N   0O   2    0G   300.000  5000.000 1682.000    01
 5.98567026E+00 9.76305949E-04-3.67418941E-07 6.09823760E-11-3.71055278E-15    2
 1.02856449E+04-8.31833092E-01 5.06381486E+00 2.94867142E-03-1.81698983E-06    3
 4.80823618E-10-4.02557747E-14 1.06037780E+04 4.15563337E+00                   4
```

```
CLO3      CLO3_G4.out   CL  1H   0N   0O   3G   300.000  5000.000 1407.000    01
 8.55671903E+00 1.34914053E-03-4.94913928E-07 8.05088576E-11-4.82528654E-15    2
 1.91486799E+04-1.77737893E+01 1.91755743E+00 2.15239268E-02-2.39015577E-05    3
 1.22170196E-08-2.35603309E-12 2.09546638E+04 1.61728591E+01                   4
CL2                42189CL  2               G  0300.00   5000.00  1000.00     1
 0.04274587E+02 0.03717337E-02-0.01893490E-05 0.05337465E-09-0.05057602E-13    2
-0.01331149E+05 0.02256947E+02 0.03439587E+02 0.02870774E-01-0.02385871E-04    3
 0.02892918E-08 0.02915057E-11-0.01131787E+05 0.06471359E+02                   4
H                  120186H   1               G  0300.00   5000.00  1000.00     1
 0.02500000E+02 0.00000000E+00 0.00000000E+00 0.00000000E+00 0.00000000E+00    2
 0.02547163E+06-0.04601176E+01 0.02500000E+02 0.00000000E+00 0.00000000E+00    3
 0.00000000E+00 0.00000000E+00 0.02547163E+06-0.04601176E+01                   4
HNO           WRA032498 H   1N   1O   1    0G   300.00   5000.00 1000.000    01
 3.16554762E+00 3.00005132E-03-3.94350282E-07-3.85787491E-11 7.08091931E-15    2
 1.18052184E+04 7.64764695E+00 4.53525882E+00-5.68546910E-03 1.85199976E-05    3
-1.71883674E-08 5.55833090E-12 1.16506820E+04 1.74314734E+00 1.28824477E+04    4
HONO               31787H   1N   1O   2     G  0300.00   5000.00  1000.00     1
 0.05486893E+02 0.04218065E-01-0.01649143E-04 0.02971877E-08-0.02021148E-12    2
-0.01126865E+06-0.02997002E+02 0.02290413E+02 0.01409922E+00-0.01367872E-03    3
 0.07498780E-07-0.01876905E-10-0.01043195E+06 0.01328077E+03                   4
NNH                120186N   2H   1          G  0250.00   4000.00  1000.00     1
 0.04415342E+02 0.01614388E-01-0.01632894E-05-0.08559846E-09 0.01614791E-12    2
 0.02788029E+06 0.09042888E+01 0.03501344E+02 0.02053587E-01 0.07170410E-05    3
 0.04921348E-08-0.09671170E-11 0.02833347E+06 0.06391837E+02                   4
HNJNO2    HNJNO2_G4.chk H   1N   2O   2    0G   300.000  5000.000 1393.000    11
 8.58829360E+00 3.55783685E-03-1.37988061E-06 2.34140297E-10-1.42057446E-14    2
 2.48692567E+04-1.72810309E+01 2.38719149E+00 2.06880667E-02-1.97118815E-05    3
 9.16137562E-09-1.66604445E-12 2.67339286E+04 1.50451867E+01                   4
HNOJNO2   HNOJNO2_B3d_B3H   1N   2O   3    0G   300.000  5000.000 1392.000    01
 1.03253946E+01 4.98675264E-03-1.80524376E-06 2.92271754E-10-1.73600960E-14    2
 1.02125162E+04-2.57969338E+01 2.76417845E+00 2.48231368E-02-2.20842798E-05    3
 9.81343839E-09-1.73206394E-12 1.26074164E+04 1.40188663E+01                   4
OH          Sand/Rusc01 O   1H   1          G  0300.00   5000.00  1000.00     1
 0.02882730E+02 0.01013974E-01-0.02276877E-05 0.02174684E-09-0.05126305E-14    2
 0.03672089E+05 0.05595712E+02 0.03637266E+02 0.01850910E-02-0.01676165E-04    3
 0.02387203E-07-0.08431442E-11 0.03391983E+05 0.01358860E+02                   4
HO2         McB93/WRA00 H   1O   2    0    0G   300.00   5000.00 1000.000    01
 4.17228728E+00 1.88117647E-03-3.46277408E-07 1.94657853E-11 1.76254294E-16    2
 2.13417795E+02 2.95767746E+00 4.30179801E+00-4.74912051E-03 2.11582891E-05    3
-2.42763894E-08 9.29225124E-12 4.46415539E+02 3.71666245E+00 1.66125750E+03    4
H2                 121286H   2               G  0300.00   5000.00  1000.00     1
 0.02991423E+02 0.07000644E-02-0.05633829E-06-0.09231578E-10 0.01582752E-13    2
-0.08350340E+04-0.01355110E+02 0.03298124E+02 0.08249442E-02-0.08143015E-05    3
-0.09475434E-09 0.04134872E-11-0.01012521E+05-0.03294094E+02                   4
NH2                McB93 N   1H   2    0    0G   300.00   5000.00 1000.000    01
 2.84768992E+00 3.14280035E-03-8.98641458E-07 1.30318284E-10-7.48812926E-15    2
 2.18239049E+04 6.47165433E+00 4.20556857E+00-2.13561363E-03 7.26851301E-06    3
-5.93069876E-09 1.80690978E-12 2.15352231E+04-1.46662770E-01 2.27475415E+04    4
NH2O        M/JB86      N   1H   2O   1    0G   300.000  5000.000 1398.000    01
 4.26222939E+00 4.60071183E-03-1.52686779E-06 2.32081624E-10-1.32607907E-14    2
 6.26937941E+03 1.89523882E+00 2.62132814E+00 8.05594293E-03-4.34199752E-06    3
 1.31067689E-09-1.79413169E-13 6.89825870E+03 1.08768221E+01                   4
N2H2       RB91/Gurvich N   2H   2    0    0G   300.00   5000.00 1000.00     01
 1.43773356E+00 8.72166734E-03-2.99323466E-06 4.50029732E-10-2.50422693E-14    2
 2.22727357E+04 1.57453260E+01 4.74387065E+00-9.15242446E-03 3.35349897E-05    3
-3.22086920E-08 1.06734098E-11 2.17525597E+04 7.28947240E-01 2.29978160E+04    4
H2NNO2          RE-FIT  0H   2N   2O   2    0G   300.000  4500.000 1000.00     01
 9.45441628E+00 3.80055304E-03-5.10139330E-07-7.97079347E-11 1.62415349E-14    2
-3.15945020E+03-2.53962326E+01 4.51412708E-01 3.07305455E-02-3.94054223E-05    3
 3.29329026E-08-1.20280756E-11-5.00637573E+02 2.13188362E+01                   4
```

```
H2O                20387H   2O   1          G  0300.00   5000.00  1000.00      1
 0.02672146E+02 0.03056293E-01-0.08730260E-05 0.01200996E-08-0.06391618E-13    2
-0.02989921E+06 0.06862817E+02 0.03386842E+02 0.03474982E-01-0.06354696E-04    3
 0.06968581E-07-0.02506588E-10-0.03020811E+06 0.02590233E+02                   4
NH3                121386N   1H   3          G  0300.00   5000.00  1000.00      1
 0.02461904E+02 0.06059166E-01-0.02004977E-04 0.03136003E-08-0.01938317E-12    2
-0.06493270E+05 0.07472097E+02 0.02204352E+02 0.01011476E+00-0.01465265E-03    3
 0.01447235E-06-0.05328509E-10-0.06525488E+05 0.08127138E+02                   4
N2H3          DB00/RB91 N   2H   3    0    0G   300.000  5000.000 1385.000    11
 5.56523220E+00 5.92789098E-03-2.05378972E-06 3.21563158E-10-1.87648230E-14    2
 2.40692822E+04-7.11150205E+00 1.68398813E+00 1.46455461E-02-9.84764677E-06    3
 3.66967922E-09-5.99668094E-13 2.54978433E+04 1.39338819E+01 2.65708384E+04    4
OJHNH3    OJHNH3_BK1_G4 CL  0H   4N   1O   1G   300.000  5000.000 1417.000    01
 6.15176103E+00 7.14174114E-03-2.20334210E-06 3.17596288E-10-1.74502751E-14    2
-7.40333472E+03-8.02764592E+00 4.08435736E+00 1.29576297E-02-8.64359256E-06    3
 3.57714495E-09-6.41625626E-13-6.77692096E+03 2.73636599E+00                   4
N2H4      BOZ_JPCA114_62H   4N   2    0    0G   300.000  5000.000 1390.000    11
 5.02599050E+00 8.65302984E-03-2.93055474E-06 4.51741564E-10-2.60716879E-14    2
 8.97814993E+03-3.92585332E+00 1.56439782E+00 1.55016475E-02-8.06079743E-06    3
 2.24077977E-09-2.80712108E-13 1.03609178E+04 1.51984751E+01                   4
DINH3     DINH3_BK1_1ROTCL  0H   6N   2O   0G   300.000  5000.000 1429.000    11
 6.21669185E+00 1.12895910E-02-3.52568970E-06 5.12341681E-10-2.83064658E-14    2
-1.42344846E+04-1.29402375E+00 6.79429066E+00 8.88257950E-03-5.13900006E-07    3
-1.00249924E-09 2.43225926E-13-1.42762170E+04-3.93519667E+00                   4
NO                 MCB93 N   1O   1    0    0G   300.00   5000.00 1000.000     01
 3.26071234E+00 1.19101135E-03-4.29122646E-07 6.94481463E-11-4.03295681E-15    2
 9.92143132E+03 6.36900518E+00 4.21859896E+00-4.63988124E-03 1.10443049E-05    3
-9.34055507E-09 2.80554874E-12 9.84509964E+03 2.28061001E+00 1.09770882E+04    4
NO2                121286N   1O   2          G  0300.00   5000.00  1000.00      1
 0.04682859E+02 0.02462429E-01-0.01042259E-04 0.01976902E-08-0.01391717E-12    2
 0.02261292E+05 0.09885985E+01 0.02670600E+02 0.07838501E-01-0.08063865E-04    3
 0.06161715E-07-0.02320150E-10 0.02896291E+05 0.01161207E+03                   4
N2                 121286N   2              G  0300.00   5000.00  1000.00      1
 0.02926640E+02 0.01487977E-01-0.05684761E-05 0.01009704E-08-0.06753351E-13    2
-0.09227977E+04 0.05980528E+02 0.03298677E+02 0.01408240E-01-0.03963222E-04    3
 0.05641515E-07-0.02444855E-10-0.01020900E+05 0.03950372E+02                   4
O                  120186O   1              G  0300.00   5000.00  1000.00      1
 0.02542060E+02-0.02755062E-03-0.03102803E-07 0.04551067E-10-0.04368052E-14    2
 0.02923080E+06 0.04920308E+02 0.02946429E+02-0.01638166E-01 0.02421032E-04    3
-0.01602843E-07 0.03890696E-11 0.02914764E+06 0.02963995E+02                   4
O2                 121386O   2              G  0300.00   5000.00  1000.00      1
 0.03697578E+02 0.06135197E-02-0.01258842E-05 0.01775281E-09-0.01136435E-13    2
-0.01233930E+05 0.03189166E+02 0.03212936E+02 0.01127486E-01-0.05756150E-05    3
 0.01313877E-07-0.08768554E-11-0.01005249E+05 0.06034738E+02                   4
END
```

INTENTIONALLY LEFT BLANK.

Appendix C. The Molecular Structures of Species in Mechanism R2

Because the CHEMKIN II framework limits the labels for species to 16 or fewer characters and many of the species are radicals or "unusual", in most cases it is not possible to assign a label (such as a SMILES [simplified molecular-input line-entry system] string) that could be unambiguously translated into a molecular structure. Correspondences between the labels and the molecular structures for which the stoichiometry and (single) mandate that hydrogen atoms only form single bonds are not sufficient to yield an unambiguous interpretation are provided in Table C-1.

Table C-1 The molecular structures of species in mechanism R2[a]

Label	Stoichiometry	Structure
CHO	CHO	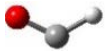
CH2O	CH_2O	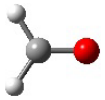
CO2	CO_2	
C2H2	C_2H_2	
C2H3	$^2C_2H_3$	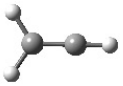
C*CCL*O	C_3ClH_3O	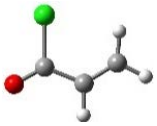
VCDJO	$^2C_3H_3O$	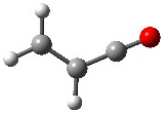
VCDO	C_3H_4O	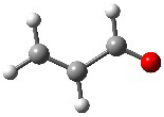
CTCV	C_4H_4	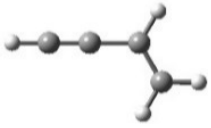
CDCCDCJ	$^2C_4H_5$	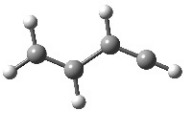

CDCCDC	C_4H_6	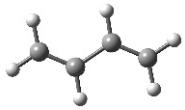
CCDOV	C_4H_6O	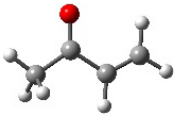
CDCCJC	$^2C_4H_7$	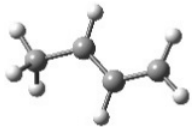
VCOJC	$^2C_4H_7O$	
CJVV	$^2C_5H_7$	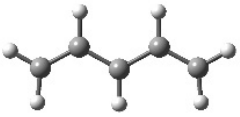
VVCOJ	$^2C_5H_7O$	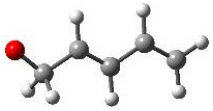
CVV	C_5H_8	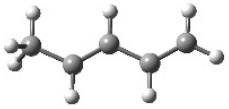
CJCVC	$^2C_5H_9$	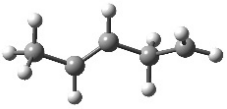
CVCCVCL	C_8ClH_{13}	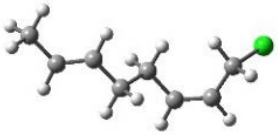
VY6DE13J	$^2C_8H_9$	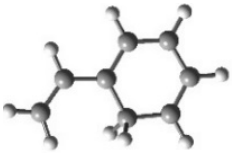

VVVJV	$^{2}C_{8}H_{9}$	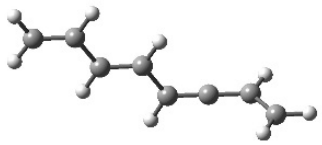
VVVIV	$C_{8}H_{10}$	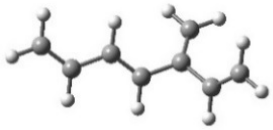
VY6DE13	$C_{8}H_{10}$	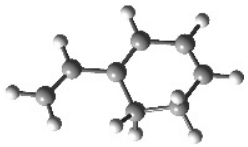
CVCZCVCJ	$^{2}C_{8}H_{13}$	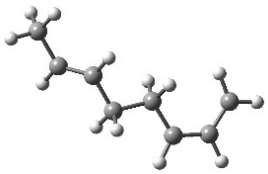
CVCCCOJV	$^{2}C_{8}H_{13}O$	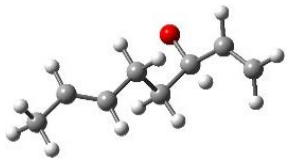
CJCVCCVC	$^{2}C_{9}H_{15}$	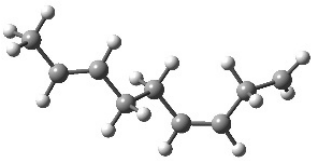
CVCCVCCOJ	$^{2}C_{9}H_{15}O$	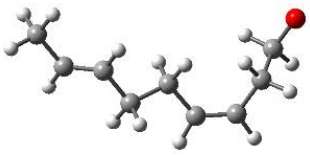
BZBCCLV	$C_{12}ClH_{19}$	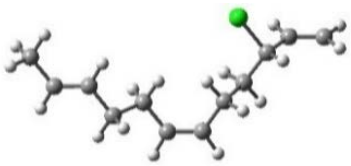
BZBBJ	$^{2}C_{12}H_{19}$	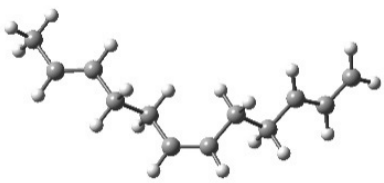

BZBCCOJV	$^{2}C_{12}H_{19}O$	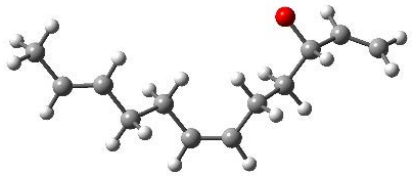
BBBCJV	$^{2}C_{15}H_{23}$	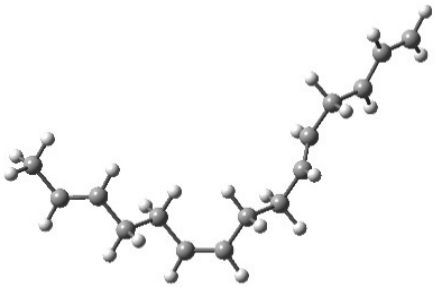
BBBCOJV	$^{2}C_{15}H_{23}O$	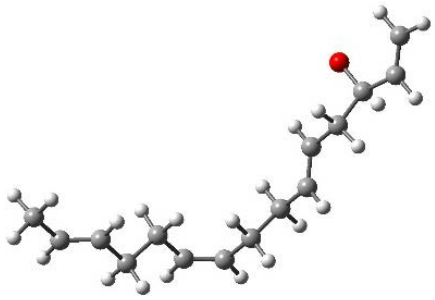
BBBJVIV	$^{2}C_{16}H_{23}$	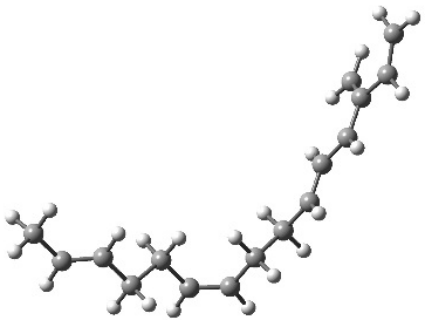
BBBVIV	$C_{16}H_{24}$	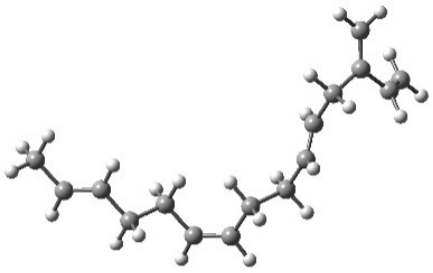

R45MLSJ	$^2C_{20}ClH_{32}$	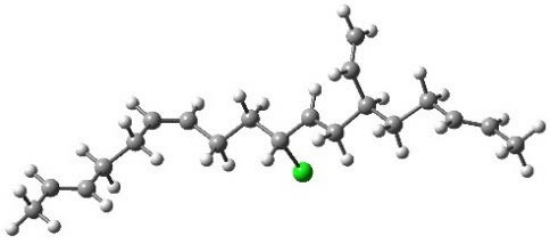
R45MLPJ	$^2C_{20}ClH_{32}$	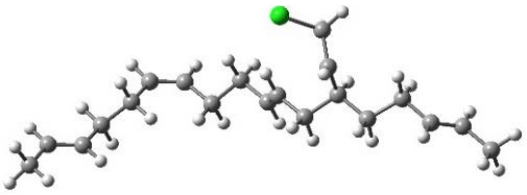
R45M9J	$^2C_{20}H_{31}$	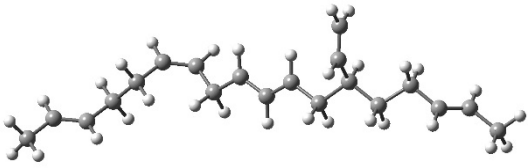
R45M13J	$^2C_{20}H_{31}$	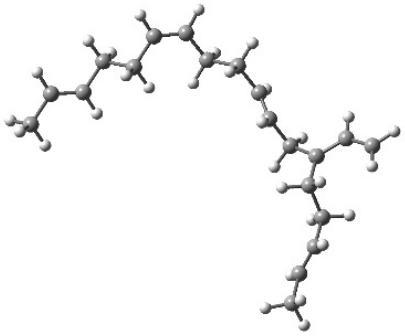
R45M	$C_{20}H_{32}$	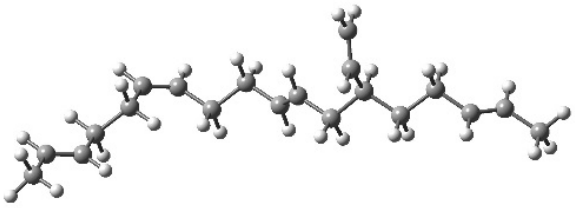
CLOH	ClHO	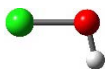
HOCLO	$ClHO_2$	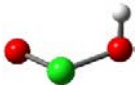
HOOCL	$ClHO_2$	

HOCLO2	$ClHO_3$	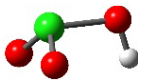
HCLO4	$ClHO_4$	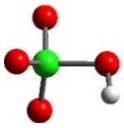
NH4CLO4	ClH_4NO_4	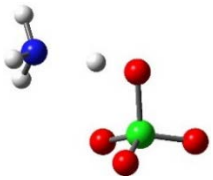
AP_NH3	$ClH_7N_2O_4$	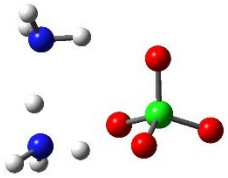
NOCL	ClNO	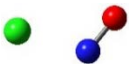
ONOCLO3	$ClNO_5$	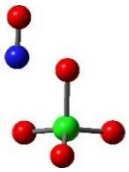
CLO2	$^2ClO_2$	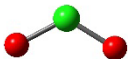
CLOO	$^2ClO_2$	
CLO3	$^2ClO_3$	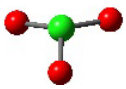
HNO	HNO	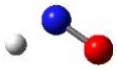
HONO	HNO_2	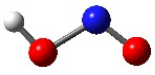
HNJNO2	$^2HN_2O_2$	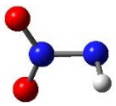
HNOJNO2	$^2HN_2O_3$	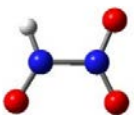

NH2O	$^{2}H_2NO$	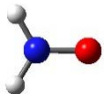
N2H2	H_2N_2	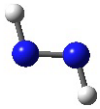
H2NNO2	$H_2N_2O_2$	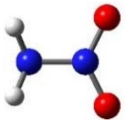
N2H3	$^{2}H_3N_2$	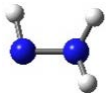
OJHNH3	$^{2}H_4NO$	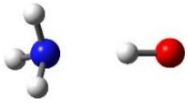
N2H4	H_4N_2	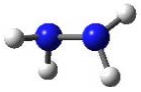
DINH3	H_6N_2	

[a]carbon (C) atoms = gray; hydrogen (H) atoms = white; nitrogen (N) atoms = blue; oxygen (O) atoms = red; and chlorine (Cl) atoms = green.

Appendix D. Parameters Employed For Computing Transport Property Estimates for Species in Mechanism R2

Table D-1 provides values for the coefficients employed to estimate the transport properties of pure species in mechanism R2. For each species/molecule, there is a set that includes 1) an index indicating whether it is monatomic, linear, or nonlinear, 2) its Lennard-Jones potential well depth (ε/k_B), 3) its Lennard-Jones collision diameter (σ), 4) its dipole moment (μ), 5) its polarizability (α), and 6) its rotational relaxation collision number (Z_{rot}).

Table D-1 Transport parameters for species in mechanism R2

Label		ε/k_B	σ	μ	α	Z_{rot}	Remarks/Reference
CHO	2	71.4	3.798	0	0	1	CHO: Chemkin (same as HCO)
CH2O	2	498	3.590	0	0	2	CH2O: Chemkin
CH3	1	144	3.800	0	0	0	CH3: Chemkin
CO	1	98.1	3.650	0	1.95	1.8	CO: Chemkin
CO2	1	244	3.763	0	2.65	2.1	CO2: Chemkin
C2H2	1	209	4.100	0	0	2.5	C2H2: Chemkin
C2H3	2	209	4.100	0	0	1	C2H3: Chemkin
C*CCL*O	2	445	4.890	0	0	1	C3ClH3O: Assume similar to CH3CH2NO2 (Tb=387K; Vb=71 cm3/mol)
VCDJO	2	425	4.970	0	0	1	C3H3O: Assume similar to 1-propanol (Tb=370K;Vb=75 cm3/mol)
VCDO	2	425	4.970	0	0	1	C3H4O: Assume similar to 1-propanol (Tb=370K;Vb=75 cm3/mol)
CTCV	2	357	5.180	0	0	1	C4H4: (= C4H4 in Chemkin)
CDCCDCJ	2	357	5.176	0	0	1	C4H5: (= C4H6 in Chemkin)
CDCCDC	2	357	5.176	0	0	1	C4H6: Chemkin
CCDOV	2	428	5.320	0	0	1	C4H6O: Assume similar to 2-butanol (Tb=372K;Vb=92 cm3/mol)
CDCCJC	2	357	5.176	0	0	1	C4H7 (=C4H6 in Chemkin)
VCOJC	2	428	5.320	0	0	1	C4H7O: Assume similar to 2-butanol (Tb=372K;Vb=92 cm3/mol)
CJVV	2	348	5.650	0	0	1	C5H7: Assume similar to 1-pentene (Tb=303K;Vb=110 cm3/mol)
VVCOJ	2	473	5.630	0	0	1	C5H7O: Assume similar to 1-pentanol (Tb=411K;Vb=109 cm3/mol)
CVV	2	362	5.470	0	0	1	C5H8: 1,3-pentadiene (Tb=315K;Vb=99.7 cm3/mol)
CJCVC	2	362	5.470	0	0	1	C5H9: Assume similar to 1,3-pentadiene (Tb=315K;Vb=99.7 cm3/mol)

Table D-1 Transport parameters for species in mechanism R2 (continued)

Label		ε/k_B	σ	μ	α	Z_{rot}	Remarks/Reference
CVCCVCL	2	524	6.540	0	0	1	C8ClH13: 1-chlorooctane (Tb=456K;Vb=170 cm3/mol)
VY6DE13J	2	470	5.860	0	0	1	C8H9: Assume similar to ethylbenzene(Tb=409K;Vb=122 cm3/mol)
VVVIV	2	451	6.440	0	0	1	C8H10: Assume similar to 3-methylheptane (Tb=392K;Vb=162 cm3/mol)
VY6DE13	2	470	5.860	0	0	1	C8H10: Assume similar to ethylbenzene(Tb=409K;Vb=122 cm3/mol)
CVCZCVCJ	2	458	6.440	0	0	1	C8H13: Assume similar to octane (Tb=399K;Vb=162 cm3/mol)
CVCCCOJV	2	520	6.390	0	0	1	C8H13O: Assume similar to 2-octanol (Tb=452K;Vb=159 cm3/mol)
CJCVCCVC	2	488	6.650	0	0	1	C9H15: Assume similar to nonane (Tb=424K;Vb=179 cm3/mol)
CVCCVCCOJ	2	560	6.590	0	0	1	C9H15O: Assume similar to 1-nonanol (Tb=487K;Vb=174 cm3/mol)
BZBCCLV	2	601	7.170	0	0	1	C12ClH19: Assume similar to 2-dodecanol (Tb=523K;Vb=225 cm3/mol)
BZBBJ	2	564	7.200	0	0	1	C12H19: Assume similar to dodecane (Tb=490K;Vb=227 cm3/mol)
BZBCCOJV	2	601	7.170	0	0	1	C12H19O: Assume similar to 2-dodecanol (Tb=523K;Vb=225 cm3/mol)
BBBCJV	2	624	7.530	0	0	1	C15H23: Assume similar to pentadecane (Tb=543K;Vb=260 cm3/mol)
BBBCOJV	2	658	7.680	0	0	1	C15H23O: Assume similar to 1-pentadecanol (Tb=572K;Vb=276 cm3/mol)
BBBJVIV	2	644	7.850	0	0	1	C16H23: Assume similar to cetane (Tb=560K;Vb=294 cm3/mol)
BBBVIV	2	644	7.850	0	0	1	C16H24: Assume similar to cetane (Tb=560K;Vb=294 cm3/mol)
R45MLSJ	2	742	8.140	0	0	1	C20ClH32: Assume similar to icosanol (Tb=645K;Vb=355 cm3/mol)
R45MLPJ	2	742	8.140	0	0	1	C20ClH32: Assume similar to icosanol (Tb=645K;Vb=355 cm3/mol)
R45M9J	2	708	8.380	0	0	1	C20H31: Assume similar to icosane (Tb=616K;Vb=358 cm3/mol)
R45M13J	2	708	8.380	0	0	1	C20H31: Assume similar to icosane (Tb=616K;Vb=358 cm3/mol)
R45M	2	708	8.380	0	0	1	C20H32: Assume similar to icosane (Tb=616K;Vb=358 cm3/mol)
CL	0	130.8	3.613	0	0	1	Cl: Chemkin 2002
HCL	1	344.7	3.339	0	0	1	ClH: Chemkin 2002
CLOH	2	430	3.690	1.844	0	1	ClHO: Tb(est)=374K; Tb(H2O)=373K (McQuaid and Chen 2014)
HOCLO	2	469	3.920	1.844	0	1	ClHO2: Tb(est)=408K (McQuaid and Chen 2014)
HOOCL	2	469	3.920	1.844	0	1	ClHO2: Assume same as HOClO (McQuaid and Chen 2014)
HOCLO2	2	508	4.120	1.844	0	1	ClHO3: Tb(est)=442K (McQuaid and Chen 2014)

Table D-1 Transport parameters for species in mechanism R2 (continued)

Label		ε/k_B	σ	μ	α	Z_{rot}	Remarks/Reference
HCLO4	2	547	4.310	1.844	0	1	ClHO4: Tb(meas)=476K[1]
NH4CLO4	2	547	4.770	0	0	1	ClH4NO4: Tb(est)=476K=Tb(HCLO4, est) (McQuaid and Chen 2014)
AP_NH3	2	547	4.770	0	0	1	ClH7N2O4: Assume similar to NH4ClO4
NOCL	2	450	3.880	0	0	1	ClNO: Svelha 1995; delta=0.50
ONOCLO3	2	547	4.770	0	0	1	ClNO5: Assume similar to NH4ClO4
CLO	1	288	3.690	0	0	1	ClO: Tb(est)=250K; Tb(SO)=262 K;Tb(Cl2)=239 K; Vb=Vb(CLOH)
CLO2	2	327	3.920	0	0	1	ClO2: Tb(meas)=284K;Vb=Vb(HOCLO)
CLOO	2	308	3.920	0	0	1	ClO2: Tb(est)=268K = Tb(NOCL); Vb=V(HOCLO)
CLO3	2	366	4.120	0	0	1	ClO3: Tb(est)=318 K; Tb(SO3)=318 K; Vb=V(HOCLO2)
CL2	1	300	4.235	0	0	1	Cl2: Svelha 1995
H	0	145	2.050	0	0	0	H: Chemkin
HNO	2	116.7	3.492	0	0	1	HNO: Chemkin
HONO	2	572.4	3.600	1.844	0	3	HNO2: from Penn State via Miller (combines parameters of H_2O and NO_2)
NNH	2	71.4	3.798	0	0	1	HN2: Chemkin
HNJNO2	2	409	4.090	0	0	1	HN2O2: Assume similar to HNO3 (Tb=356K; Vb=42 cm3/mol)
HNOJNO2	2	389	4.720	0	0	1	HN2O3: Assume similar to CH3ONO2 (Tb=338K; Vb=64 cm3/mol)
OH	1	80	2.750	0	0	0	HO: Chemkin
HO2	2	107.4	3.458	0	0	1	HO2: Chemkin
H2	1	38	2.920	0	0.79	280	H2: Chemkin
NH2	2	80	2.650	0	2.26	4	H2N: Chemkin
NH2O	2	116.7	3.492	0	0	1	H2NO: Assume similar to HNO
N2H2	2	71.4	3.798	0	0	1	H2N2: Chemkin
H2NNO2	2	430	3.810	0	0	1	H2N2O2: Nitramide. Tb(est)=374K; Vb(Klapotke)=34 cm3/mol)
H2O	2	572.4	2.605	1.844	0	4	H2O: Chemkin
NH3	2	481	2.920	1.47	0	10	H3N: Chemkin
N2H3	2	200	3.900	0	0	1	H3N2: Chemkin
OJHNH3	2	381	3.550	0	0	1	H4NO: Assume similar to NH2OH (Tb=331K; Vb=27.6 cm3/mol)

[1]McQuaid MJ, Chen CC. Modeling the deflagration of ammonium perchlorate at pressures from 300 to 30000 psia. Part II: considerations besides the gas-phase, finite-rate chemical kinetics mechanism. Presented at the 46th JANNAF Combustion Subcommittee Meeting; 2014 Dec 8–11; Albuquerque, NM.

Table D-1 Transport parameters for species in mechanism R2 (continued)

Label		ε/k_B	σ	μ	α	Z_{rot}	Remarks/Reference
N2H4	2	205	4.230	0	4.26	1.5	H4N2: Chemkin
DINH3	2	276	4.350	0	0	1	H6N2: Assume Tb=Tb(NH3)=240K; Vb=2*Vb(NH3)=50 cm3/mol
NO	1	97.53	3.621	0	1.76	4	NO: Chemkin
NO2	2	200	3.500	0	0	1	NO2: Chemkin
N2	1	97.53	3.621	0	1.76	4	N2: Chemkin
O	0	80	2.750	0	0	0	O: Chemkin
O2	1	107.4	3.458	0	1.6	3.8	O2: Chemkin

Except for the index indicating whether a molecule is monatomic, linear, or nonlinear, for all but common combustion products, values for these parameters are not obvious or obtainable from open literature sources and have to be estimated. While this has the potential to be an arduous task,[2] we found negligible differences in burning rate estimates for pure ammonium perchlorate produced when a set for a relatively small and nonpolar molecule such as CH_3CHO was employed for all unknowns and when the sets included first-order approximations for ε/k_B and σ and a value for μ = 1.844 (instead of zero) if the molecule had a hydroxyl group (McQuaid and Chen 2014). Concluding that obtaining first-order approximations for ε/k_B and σ was adequate for our purposes, we employed that approach to estimate values for species in mechanism R2.

For species for which established estimates for ε/k_B, σ, μ, α, and Z_{rot} could not be found, we followed past practice: setting α = 0 and Z_{rot} = 1.0. If the molecule had a hydroxyl group, μ was set equal to 1.844 (i.e., the μ for H_2O). Otherwise it was set equal to 0.

Estimates for ε/k_B and σ were obtained via

$$\varepsilon/k_B = 1.15 * T_b,$$

where T_b is the species' normal boiling point and

$$\sigma = 1.18 * V_b^{1/3},$$

where V_b is the species' molecular volume at the normal boiling point (Welty et al. 1976).[3] Values for T_b and V_b were obtained via an internet search. Wikipedia was typically consulted first. If it did not yield a suitable result, the Sigma-Aldrich catalog and/or www.nbchem.ncbi.nlm.nih.gov were searched. None of the T_b and V_b values that were found had formal attribution. Our only criteria for employing a value was that it conform to our expectations for the relative values of species based on molecular size and the presence of certain functional groups. Moreover, in the majority of cases (including most radicals), T_b and V_b for the molecule/species of specific interest could not be (nor could they be expected to be) found. In these cases, values for a species of similar elemental composition/size and polarity were sought and used.

[2]Troe, J. Theory of thermal unimolecular reactions at low pressures: II. strong collision rate constants: applications. Journal of Physical Chemistry. 1977;66:4758.

[3]Welty JR, Wicks CE, Wilson RE. Fundamentals of momentum, heat, and mass transfer. New York (NY): John Wiley and Sons; 1976.

List of Symbols, Abbreviations, and Acronyms

1-D	1-dimensional
AP-HTPB	ammonium perchlorate–hydroxyl-terminated polybutadiene
ARL	US Army Research Laboratory
CFD	computational fluid dynamics
CONP	constant pressure
DFT	density functional theory
HR	homogeneous reactor
MR	microscopic reversibility
TMM	trial mechanism method
TST	transition state theory
VTST	variational transition state theory
$\dot{m}$	mass flux rate
r_b	burning rate
T_s or T^0	temperature at burner surface/condensed-phase—gas-phase interface

1 (PDF) DEFENSE TECHNICAL INFORMATION CTR DTIC OCA

2 (PDF) DIRECTOR US ARMY RESEARCH LAB RDRL CIO LL IMAL HRA MAIL & RECORDS MGMT

1 (PDF) GOVT PRINTG OFC A MALHOTRA

2 (PDF) ARMY RSRCH OFC CHEMICAL SCI DIV R ANTHENIEN J PARKER

11 (PDF) US ARMY AVN & MIS CMND RDMR WDP P S BOLDEN J DAILEY R ESSLINGER G DRAKE N MATHIS R MICHAELS J NEIDERT L PLEDGER

1 (PDF) US NAVAL RES LAB CODE 6189 I SCHWEIGERT

1 (PDF) TEXAS A&M UNIV DEPT MECH ENGINEERING E PETERSEN

1 (PDF) CAL TECH CHEMISTRY & APPLIED PHYSICS W GODDARD

1 (PDF) EMORY UNIV DEPT CHEMISTRY M LIN

3 (PDF) PENN STATE CENTER FOR COMB PROP & POWER S THYNELL R YETTER VAN DUIN

1 (PDF) NC STATE DEPT CHEM & BIOMECH ENG P WESTMORELAND

1 (PDF) PURDUE UNIV SCHOOL AERONAUT & ASTRONAUT S SON

1 (PDF) NEW JERSEY INST TECH DEPT CHEM & ENVIRON SCI J BOZZELLI

1 (PDF) MASS INST TECH CHEMICAL ENGRNG W GREEN

1 (PDF) BROWN UNIV SCHOOL OF ENGRNG C GOLDSMITH

1 (PDF) PRINCETON UNIV MECH & AEROSPACE ENG C LAW

1 (PDF) UNIV MISSOURI-COLUMBIA DEPT OF CHEMISTRY D THOMPSON

1 (PDF) UNIV MASSACHUSETTS-BOSTON COLLEGE OF SCIENCE & MATH J GREEN

2 (PDF) NAWCWD-CHINA LAKE M GROSS A ATWOOD

1 (PDF) SANDIA NATIONAL LAB J KAY

27 (22 PDF 5 HC) DIR USARL RDRL WM B FORCH RDRL WML M ZOLTOSKI RDRL WML A W OBERLE RDRL WML B J BRENNAN E BYRD J CIEZAK-JENKINS B RICE D TAYLOR N TRIVEDI RDRL WML C S AUBERT RDRL WML D R BEYER C CHEN

M MCQUAID (5 HC, 1 PDF)
M NUSCA
J VEALS
RDRL WML E
P WEINACHT
RDRL WML F
M ILG
RDRL WML G
J SOUTH
RDRL WML H
J NEWILL
RDRL WMM G
J ANDZELM
T CHANTAWANSRI
RDRL VTD
L BRAVO ROBLES

INTENTIONALLY LEFT BLANK.